科技部補助專題研究計畫成果報告
期末報告

探討斑馬魚di-ras基因及其相關基因在神經發育所扮演的角色

計 畫 類 別 ： 個別型計畫
計 畫 編 號 ： MOST 103-2311-B-040-001-
執 行 期 間 ： 103年08月01日至104年07月31日
執 行 單 位 ： 中山醫學大學生化暨生物科技研究所

計 畫 主 持 人 ： 許立松

計畫參與人員： 碩士級-專任助理人員：李宜勳

報 告 附 件 ： 出席國際會議研究心得報告及發表論文

處 理 方 式 ：
1.公開資訊：本計畫涉及專利或其他智慧財產權，2年後可公開查詢
2.「本研究」是否已有嚴重損及公共利益之發現：否
3.「本報告」是否建議提供政府單位施政參考：否

中 華 民 國 104 年 11 月 02 日

中 文 摘 要 ： 小G蛋白ras家族可以調控許多生理功能包含神經分化以及神經生長。在此研究我們發現斑馬魚的diras1a以及diras1b基因主要分布在中樞神經以及背部神經管。大量表現diras1a以及diras1b會促進Neuro-2A細胞神經分化透過增加Rac1並降低RhoA的表現。GST-pull down方法亦證實diras1會促進Rac1的活性。將Rac1, PAK, CDK5cji4g4ARP2/3抑制劑可以減少diras1促進Neuro-2A細胞神經分化的現象。在斑馬魚中利用morpholino反譯股核酸去抑制diras1a或是diras1b表現會減少trigeminal ganglion數目但是不會影響早期身經標誌如Neuro D或是ngn1表現。利用老鼠diras1基因或是持續活化泰的Rac1基因可以彌補抑制diras1a或是diras1b所引起的現象。總結：我們實驗證實斑馬魚中diras基因確實可以透過Rac1途徑參與trigeminal ganglion神經分化的作用。

中 文 關 鍵 詞 ： 斑馬魚diras1基因; 神經發育;基因剃除

英 文 摘 要 ：

英 文 關 鍵 詞 ：

Zebrafish *diras1* promoted neurite outgrowth in Neuro-2a cells and maintained trigeminal ganglion neurons *in vivo* via Rac1-dependent pathway

Chi-Wei Yeh[1], Li-Sung Hsu[1,2*]

1 Institute of Biochemistry and Biotechnology, Chung Shan Medical University, Taichung, 40201, Taiwan

2 Clinical Laboratory, Chung Shan Medical University Hospital, Taichung, 40201, Taiwan

*: To whom correspondence should be addressed, Li-Sung Hsu. Institute of Biochemistry and Biotechnology, Chung Shan Medical University, No.110, Sec.1, Jianguo N.Rd., Taichung City, 40201,Taiwan. E-mail: lshsu405@yahoo.com.tw Tel: 886-4-24730022 ext 11382 Fax: 886-4-23248195

Abstract

The small GTPase Ras superfamily regulates several neuronal functions including neurite outgrowth and neuron proliferation. In this study, zebrafish *diras1a* and *diras1b* were identified and were found to be mainly expressed in the central nervous system and dorsal neuron ganglion. Overexpression of GFP-*diras1a* or GFP-*diras1b* triggered neurite outgrowth of Neuro-2a cells. The wild types, but not the C-terminus truncated forms, of *diras1a* and *diras1b* elevated the protein level of Rac1 and downregulated RhoA expression. GST pull-down assay also revealed that *diras1a* and *diras1b* enhanced Rac1 activity. Interfering with Rac1, Pak1, or CDK5 activity or with the Arp2/3 inhibitor prevented *diras1a* and *diras1b* from mediating the neurite outgrowth effects. In the zebrafish model, knockdown of *diras1a* and/or *diras1b* by morpholino antisense oligonucleotides not only reduced axon guidance but also caused the loss of trigeminal ganglion without affecting the precursor markers, such as *ngn1* and *neuroD*. Co-injection with mRNA derived from mouse *Diras1* or constitutively active human *Rac1* restored the population of trigeminal ganglion. In conclusion, we provided preliminary evidence that *diras1* is involved in neurite outgrowth and maintains the number of trigeminal ganglions through the Rac1-dependent pathway.

Keyword: diras1, neurite outgrowth, rac1, trigeminal ganglion, zebrafish

Introduction

The Ras GTPase superfamily proteins function as important regulators in a wide variety of biological processes, including proliferation, differentiation, signal transduction, protein synthesis, and cell metabolism [1-3]. The Ras superfamily is divided into five subfamilies according to their sequence homology and biochemical properties. The five families are Ras, Rho, Rab, Ran, and Arf [3]. The Ras superfamily switches between two states, namely, a GTP-bound active form and a GDP-bound inactive form. The activation of Ras proteins is mediated by guanine nucleotide exchange factors that facilitate the exchange of the GDP-bound form and is deactivated by GTPase-activating proteins that enhance intrinsic GTP hydrolysis. When bound to GTP, Ras proteins associate with effectors, which results in the propagation of downstream signaling [4,5].

Recent evidence suggests that Rho subfamily proteins are key regulators of the actin cytoskeleton, cell adhesion [6,7], and cell polarization [8]. The most understood proteins in the Rho-family GTPase are Ras-related C3 botulinum toxin substrate 1 (Rac1), cell division cycle 42 (cdc42), and Ras homologous member A (RhoA). Rac1 induces lamellipodium formation through actin polymerization, Cdc42 regulates the formation of filopodia [9,10], and RhoA mediates stress fiber formation [11]. These three Rho family GTPases, which may be involved in neuron development, are predominantly expressed throughout the nervous system in such areas as the hippocampus, cerebellum, thalamus, and neocortex [12]. Emerging reports indicate that Rho GTPases regulate the axonal initiation and motility of

neurite terminals. Rac1 and Cdc42 generally serve as positive regulators that promote neurite growth [13,14], whereas RhoA activation appears to serve as a negative regulator that suppresses neurite growth [15].

Ellis et al. and *Kontoni et al*. recently identified novel Ras members, namely, DIRAS1 and DIRAS2 proteins, which belong to a distinct subfamily of Ras GTPases [5,16]. The mRNA transcripts of *DIRAS1* and *DIRAS2* are specifically expressed in adult human brain tissues [5,16]. DIRAS1 and DIRAS2 exhibit low levels of intrinsic nucleotide hydrolysis activity and predominantly exist in a GTP-bound state [16]. The forced expression of *DIRAS1* does not affect Raf kinase and thus fails to trigger MAPK activation and Elk-1 transactivation [5,16]. DIRAS1 has been described as a potential tumor suppressor that attenuates the growth of human glioblastomas [5]. Recent evidence from the *Caenorhabditis elegans* model suggests that *drn-1*, a *DIRAS1* homologue in *C. elegans*, is restricted in neuron cells and is required for neuromuscular junctions [17].

Although *drn-1* has been shown to modulate synaptic activity in motor neurons [17], the biological function of DIRAS1 in neuron development remains uncertain. In this study, we perform functional analysis and provide evidence of the expression patterns of two zebrafish *diras1* genes: *diras1a* and *diras1b*. Both genes are predominantly expressed in the brain region and retina ganglion cells. The ectopic expression of the wild-type, but not the C-terminus truncated form, of *diras1* genes in Neuro-2a cells induces protrusion formation.

Zebrafish *diras1a* and *diras1b* are found to elevate the protein level and activities of Rac1 and attenuate RhoA expression in Neuro-2a cells. Blocking Rac1 downstream signals abrogates *diras1a*- and *diras1b*-induced neurite outgrowth. Interfering with *diras1a* and/or *diras1b* expression decreases the number of trigeminal ganglia. Co-injection of the wild-type, but not the C-terminal truncated form, of mouse *Diras1* mRNA and constitutively active *Rac1* mRNA rescues the MO-induced effects. Altogether, these data comprise the preliminary evidence highlighting the function of diras1 proteins in neuronal development.

Materials and Method

Ethics statement

All procedures involving experimental animals described in this work were approved by the Institutional Animal Care and Use Committee (IACUC Approval NO. 1344) of Chung-Shan Medical University Experimental Animal Center.

Fish maintenance

Zebrafish (*Danio rerio*) AB strains and transgenic *Tg*(*huC:gfp*) fish were provided by the Taiwan Zebrafish Core Facility (Academia Sinica, Taiwan). The fish were kept at 28 ℃ under standard conditions [18,19]. The developmental stages of the fish were determined

according to the morphological criteria described by Kimmel et al. [20].

Reagents

All chemicals were purchased from Sigma Chemical Company or J. T. Baker. Antibodies against GFP, Pak1, RhoA, Rac1, CDC42, WAVE, and Arp2/3 were purchased from Santa Cruz Biotechnology. Anti-β-actin and horseradish peroxidase (HRP)-conjugated secondary antibodies were obtained from Sigma Chemicals Company. Fetal bovine serum and penicillin–streptomycin mixture were obtained from Gibco Laboratory. Plasmids, namely, DN-Rac1 (Plasmid #20151), pcDNA3-EGFP-RhoA-Q63L (Plasmid #12968), pCMV6M-Pak1-K299R (Plasmid #12210), CDK5-DN-HA (Plasmid #1873) and pGEX-Pak1 83-149 (Plasmid #12216) were purchased from Addgene.

Isolation of zebrafish cDNAs

Total RNAs derived from the different stages were purified using TRIzol Reagent (Invitrogen) according to manufacturer's recommendations. Total RNA (5 μg) and a random primer were used for the synthesis of first-strand cDNA with MMLV reverse transcriptase (Promega). PCR amplification was performed using 1 μl of cDNA as the template and the following specific primers: wild-type zebrafish *diras1a*, 5′-GCAGCATGCCAGAGCAGAG-3′ (sense) and 5′-GGCAGCATACAAATCATGAC-3′ (anti-sense: R_1); wild-type zebrafish

diras1b, 5′-GATGCCTGAGCAGAGCAACG-3′ (sense) and 5′-GCAAGTCTACATGACACTGC-3′ (anti-sense: R_3); C-terminal truncate zebrafish *diras1a*, 5′-CTACTTGGCCTTCAGCTTGTC-3′ (anti-sense); C-terminal truncate zebrafish *diras1b*, 5′-TCATTTCCCCTTCAGCTTGTC-3′ (anti-sense); wild-type mouse *diras1*, 5′-ATGCCAGAACAGAGCAATGAC-3′ (sense) and 5′-GGGCTCACATGAGCGCGCAC-3′ (anti-sense); and C-terminal truncate mouse *diras1*, 5′-TCACTTGCCCTTGATGCGGTCAG-3′ (anti-sense). PCR was programmed as follows: denaturation at 95 ℃ for 5 min followed by 35 cycles of 94 ℃ for 30 s, 55 ℃ for 30 s, and 72 ℃ for 1 min. The final extension was at 72 ℃ for 5 min. The negative control was concomitantly prepared using water instead of cDNA. The amplification of elongation factor 1α was used as the loading control. Amplified fragments were subcloned into the pGEM-T easy and $pCS2^+$.

Morpholino oligonucleotides and mRNA injections

All morpholino antisense oligonucleotides were designed and synthesized by Gene Tools, LLC (Philomath, OR): *diras1a* MO: (5'-GGTAATCGTTACTCTGCTCTGGCAT-3'); *diras1b* MO: (5'-AGTCGTTGCTCTGCTCAGGCATCTT-3'); *diras1a*-5mis MO: (5'-GCTAATCCTTAGTCTCCTCTCGCAT-3'); *diras1b*-5mis MO: (5'-AGTCCTTCCTCTCCTCACGGATCTT-3'); *diras1a* splice MO:

(5’-AAAGCGATGTATTCTTACCTGGCGA-3’); *diras1b* splice MO: (5’-ACGTTCTAGACCTAGTAGAGAGAAA-3’); *p53* MO: (5'-GCGCCATTGCTTTGCAAGAATTG-3'); control MO: (5'-CCTCTTACCTCAGTTACAATTTATA-3') corresponding to the human β-globin gene was used as a negative control. MOs were dissolved in 1x Danieau solution and injected into the embryos at the one- to two-cell stage. Efficiencies of splice morpholinos were confirmed by PCR on cDNA derived from morpholino-injected embryos using the following primers: diras1a splice forward (Exon: F_1), 5’-TTTGGGACGTTGCAACACAG-3’; diras1a splice reverse (Intron: R_2), 5’-GGAATGCAGATATGAGATGGC-3’; diras1b splice forward (Exon: F_2), 5’-GATCAGTCACGCGGGACACG-3’; diras1b splice reverse (Intron: R_4), 5’-AAGCGGCTCTCTGTAATCGG-3’.

In situ hybridization

The entire coding sequences and partial 3′-untranslated regions of *diras1a* and *diras1b* were amplified and subcloned into the pGEM-T easy vector (Promega, USA). The digoxigenin-labeled anti-sense riboprobes for both genes were synthesized through *in vitro* transcription by SP6 RNA polymerase following the manufacturer’s standard protocol (Roche, Swiss). Whole mount *in situ* hybridization was performed as previously described [21].

Cell culture, transfection, and differentiation of neuroblastoma cells

Mouse neuroblastoma Neuro-2a cells (BCRC 60026) were purchased from Bioresource Collection and Research Center and stored in MEM supplemented with 10% fetal bovine serum, 100 μg/ml of streptomycin and 100 U/ml of penicillin. The cells were kept in a humidified 5% CO_2 incubator. Plasmid DNA was transfected into Neuro-2a cells using Lipofectamine reagent (Invitrogen, USA). The cell lysates were collected 24 h post-transfection. Morphological changes were assessed. Six to seven areas were randomly photographed from three independent experiments via LSM META 510 confocal microscopy (Zeiss). The results were compared using Student's *t*-test.

GST-pull down assay

The GST and GST-Pak1 (amino acid residues 83-149) were expressed in DH5α bacterial cells and purified according to standard procedures, as previously described [22]. The cell lysates from overexpressed cells indicated that plasmids were obtained, and protein concentrations were measured using a Bradford protein assay kit (Bio-Rad). Cell lysates (500 μg) were incubated with 5 μg of GST or GST-Pak1 (amino acids residues 83-149) fusion protein overnight at 4 ℃. After washing thrice with lysis buffer, the complexes were subjected to Western blot analysis using the specific antibody against Rac1 to determine the activated form of Rac1.

Western blot analysis

The cell lysates derived from *diras1a*- or *diras1b*-overexpressing cells were obtained. Protein (50 μg) was separated using 10% polyacrylamide gel and then transferred into nitrocellulose membranes. The membrane was blocked with phosphate-buffered saline (PBS) containing 5% nonfat milk for 1 h at room temperature. Thereafter, the membrane was probed with the indicated primary antibodies at 4 ℃ overnight. The membrane was washed with PBS containing 0.1% Tween-20 (PBST) and then reacted with HRP-conjugated secondary antibody (Santa Cruz Biotechnology). The membrane was again extensively washed with PBST, after which the reactive signal was detected using an enhanced chemiluminescence kit (Amersham Pharmacia Biotech, UK). The β-actin expression was used as the internal control.

Immunostaining

Briefly, embryos at the indicated stages were collected, fixed in 4% paraformaldehyde at 4 ℃ overnight, and then stored in methanol at −20 °C. After rehydration with PBST (PBS containing 0.1% Tween 20), the embryos were blocked with blocking solution (5% goat serum, 2% bovine serum albumin, and 1% DMSO in PBST) for 1 h and then incubated with primary antibodies at 4 ℃ overnight. Samples were washed with PBST and incubated with secondary antibodies in blocking buffer at 4 ℃ overnight in the dark. After washing with

buffer solution (2% BSA and 1% DMSO in PBST), images were captured using a scanning laser confocal microscope (510 META ZEISS). The primary antibodies include mouse anti-acetylated α-tubulin (1:1000) and rabbit anti-isl1/2 (1:200). The secondary antibodies include goat anti-mouse conjugate-FITC (1:500) and goat anti-rabbit Alexa Fluor 568 (1:500).

Results

Zebrafish *diras1a* and *diras1b* are predominantly expressed in the brain region

In previous experiments, we performed microarray analysis and identified the downstream targets of zebrafish regulator of g-protein signaling 7 (rgs7) gene, namely, calcium/calmodulin-dependent protein kinase II (cam-kii) inhibitors and cyclin-dependent protein kinase–like 1 (zcdkl1) [22,23]. In this study, we selected another putative rgs7 target (GenBank Accession No. NM-199831.1) for further investigation. The *diras1a* gene contains 2142 base pairs and encodes a polypeptide of 195 amino acid residues. In a BLASTP search of diras1a amino acids, one gene (LOC565395; GenBank Accession No.NM-001126421.1), which is highly similar to human *DIRAS1*, was found and designated as *diras1b*. The 198 amino acids encoded a diras1b protein and shared 90% identity and 95% similarity with diras1a. The homologies of the deduced amino acid sequences of diras1 and those of other species were analyzed using the CLUSTALW program

(Fig. 1A). diras1a and diras1b showed amino acid alignments similar to those from rats, mice, and humans (ranging from 80% to 87%). Motif research of the diras1 sequences showed that they contain a well-conserved guanine-nucleotide-binding domain. The G1 domain contains the GXXXXGKS motif (corresponding to Residues 14 to 21 of both genes). The invariant T of the G2 domain and the DXXG motif of G3 domain were found in Residue 39 and Residues 61 to 64, respectively. The conserved motifs NKXD in the G4 domain and EXSAK in the G5 domain were localized in Residues 121 to 124 and 148 to 152, respectively. In addition, both diras1a and diras1b contained the C-terminal CAAX (A represents aliphatic or aromatic amino acids, whereas X represents amino acid residue is critical for determine the type of covalent isoprenylation) motif, with X being a methionine. This finding suggests that both genes are putative substrates for farnesyl transferase. Based on the phylogenetic analysis, zebrafish *diras1a* and *diras1b* are members of a separate cluster (Fig. 1B). To determine whether *diras1a* and *diras1b* genes share a conserved synteny with mammalian species, we compared the gene order around *diras1a* and *diras1b* in zebrafish, humans, rats, and mice. The *diras1b* gene clustered with growth arrest and DNA-damage–induced beta (*gadd45bb*), guanine nucleotide binding protein gamma 7 (*gng7*), and silute carrier protein family 1, member 8b (*slc1a8b*). During linking, group 2 exhibited conserved synteny with the genes in human Chromosome 19, rat Chromosome 7, and mouse Chromosome 10 (Fig. 1C). *diras1a* was flanked by *adenomatous polyposis coli 2* (*apc2*) and *vitellogenin 3* (*vtg3)*. Our

results suggest that *diras1b* is a true orthologue of mammalian *DIRAS1*, whereas *diras1a* is generated from whole genome duplication. Whole mount *in situ* hybridization analysis revealed that no RNA transcripts of *diras1a* and *diras1b* were found at the 32-cell stage. At 24 h post-fertilization (hpf), *diras1a* RNA was diffusedly expressed in the brain region with high expression in the hindbrain region. By contrast, *diras1b* was weakly expressed in the brain region. At 36 hpf, *diras1a* was abundantly expressed in the olfactory bulb, ventral rostral cluster of the ventral telencephalon, hypothalamus, hindbrain, otic vesicle, and neurons in the dorsal spinal cord. At 48 hpf, *diras1a* expression was strong in the olfactory bulb, thalamus, diencephalons, otic vesicle, and midbrain, as well as in the ganglion cell layer (GCL) of the retina. Low levels of *diras1a* were also found in dorsal spinal cord neurons. At 72 hpf, *diras1a* expression was enhanced throughout the whole brain region, as well as in the GCL and inner nuclear layer of the retina (Fig. 1D). By contrast, the transcript of *diras1b* was weakly expressed in the telencephalon, diencephalon, and hindbrain at 36 hpf. At 48 hpf and 72 hpf, *diras1b* appeared in the telencephalon, diencephalon, hindbrain, and GCL of the retina (Fig. 1E).

Zebrafish *diras1a* and *diras1b* promote neurite outgrowth in Neuro-2a cells

Given that zebrafish *diras1a* and *diras1b* were specifically expressed in the neuron system, we used mouse neuroblastoma cell line Neuro-2a, which is widely employed to study

the mechanisms of neuronal differentiation, as an *in vitro* model to investigate the biological function of *diras1a* and *diras1b*. Neuro-2a cells were transfected with various GFP-tagged forms of *diras1*. At 24 h post-transfection, GFP-*diras1a* and GFP-*diras1b* were found to be localized to the plasma membrane region. By contrast, a lone GFP vector was widely expressed in whole cells. The truncated mutant GFP-*diras1a*-ct or GFP-*diras1b*-ct, which lacks the CAAX terminal membrane-anchoring motif, was also expressed diffusedly in the cells. Interestingly, Neuro-2a cells transfected with GFP-*diras1a* or GFP-*diras1b* exhibited lamellipodia-like morphological changes, as evidenced by F-actin staining (Fig. 2A). Lamellipodia-like formation is rarely observed among Neuro-2a cells with overexpressed GFP alone or in truncated mutant forms. Quantitative analysis showed that the percentage of differentiation in GFP-*diras1a*- or GFP-*diras1b*-overexpressing cells was significantly higher than that in the control groups and that C-terminal truncated form-overexpressing mutants had no effect on differentiation (Fig. 2B). Therefore, zebrafish *diras1a* and *diras1b* may promote neurite outgrowth among Neuro-2a cells.

Functions of Rac1 and RhoA in the *diras1*-induced neurite outgrowth of Neuro-2a cells

Among the signaling molecules that control cell polarity, the Rho-family small GTPases (e.g., Rac1, Cdc42, and RhoA) are characterized by their functions in regulating cytoskeletal remodeling [8,24]. To evaluate which Rho GTPases are affected by *diras1a* and *diras1b*, we

assessed the protein level using Western blot analysis. As shown in Figs. 3A and B, overexpression of GFP-*diras1a* and GFP-*diras1b* significantly increased Rac1 protein level and decreased RhoA protein expression, unlike the case of the truncated forms and control groups. However, a lack of alternation in Cdc42 expression was observed. Rac1 can reportedly induce neuronal polarization, whereas RhoA serves a critical function in collapsing the growth cone by promoting membrane retraction [25]. To elucidate further the functions of Rac1 and RhoA in *diras1*-induced neurite outgrowth, the dominant negative form of Rac1 (T17N) and constitutively activated RhoA (Q63L) were separately co-transfected with GFP-*diras1* into Neuro-2a cells. As expected, the cells with either decreased Rac1 activity or increased RhoA activity exhibited abrogated *diras1*-mediated neurite outgrowth morphology (Fig. 4A-D). Our results suggest that upregulation of Rac1 and downregulation of RhoA may be involved in *diras1*-induced neurite outgrowth. The activated GTP-bound form of Rac1/Cdc42 binds to the p21-binding domain (PBD) and subsequently increases Pak1 activities by interrupting the trans-inhibition of Pak1 [26,27]. To ascertain whether *diras1a* and *diras1b* enhances Rac1 activity, Rac1 activation status was assessed by extracting GTP-bound Rac1 proteins from cell lysates using a GST-PBD of Pak1 (amino acids residues 83-149) fusion protein. As shown in Fig. 3C, Rac1 is clearly present in lysates derived from cells that expressed GFP-*diras1a* and GFP-*diras1b*. By contrast, cells that expressed C-terminal truncated mutants relatively decreased their association with Pak1 (Fig. 3C).

These results indicate that diras1-mediated neurite outgrowth can be attributed not only to the enhanced expression but also to the increased activities of Rac1.

Zebrafish *diras1* triggers neurite outgrowth by modulating Rac1 downstream effectors

Pak1 and CDK5 have recently been implicated in neuronal cytoskeleton dynamics [28]. Both Pak1 and CDK5 are the main kinases for Rac1-mediated normal neuronal differentiation and function [29,30]. We hypothesize that Pak1 and CDK5 contribute to diras1 signaling. To test this hypothesis, the kinase-inactive dominant negative CDK5 mutant (pCMV-Mcherry-Cdk5-D145N) or the catalytically inactive form of Pak1 (pCMV-Mcherry-Pak1-K299R) was co-transfected with GFP vector alone, GFP-*diras1a*, or GFP-*diras1b* into Neuro-2a cells. The expression of kinase-negative CDK5-D145N or Pak1-K299R significantly decreased protrusion in *diras1*-overexpressing Neuro-2a cells (Figs. 4C and D). Similarly, Neuro-2a cells was transfected with inhibitory constructs alone also presence the similar pattern compare to mCherry vector alone (Supplementary Fig. 1). Accumulated evidence suggests that Rac1 relays signaling cascades to the neuronal cytoskeleton using the Wiskott-Aldrich syndrome protein (WASP) family and the verprolin-homologous protein (WAVE) family, activates actin-related protein 2/3 (Arp2/3) complex-dependent nucleation, and subsequently provides a filamentous resource to organize actin polymerization [31-33]. To validate the functions of WAVE1 and Arp2/3 in

diras1-induced polarization, Western blot analysis was conducted. As shown in Figs. 5A and B, wild types of *diras1a* and *diras1b* obviously elevated WAVE1 expression, unlike the deleted forms of *diras1a* and *diras1b* and GFP alone. However, no overt alternation of Arp2/3 expression was found. To determine whether Arp2/3 affects *diras1*-induced polarization, an Arp2/3 inhibitor was used. The *diras1*-induced polarization phenotype was significantly blocked in Neuro-2a cells pre-treated with Arp2/3 inhibitor CK-548 (Figs. 5C and D). Accordingly, our findings imply that *diras1* triggers nuerite outgrowth using the Rac1 downstream effectors.

Depletion of *diras1a* and/or *diras1b* affects neural development in zebrafish

To address the function of *diras1* in zebrafish embryogenesis, we injected antisense MOs bounded to the ATG site and blocked the translation to one-cell stage embryos to knock down *diras1a*, *diras1b*, or both. To evaluate the specificity and effectiveness of *diras1a* MO and *diras1b* MO, *diras1a*:*gfp* and *diras1b:gfp* constructs, which are composed of morpholino target sequences fused to sequences encoding GFP, were generated and co-injected with the corresponding *diras1* MO. In addition, five mismatched MOs were used as negative controls. The expression of *diras1*:*gfp* was detected in the injected embryos at 24 hpf without developmental malformation. The GFP signal was diminished in embryos injected with *diras1a* MO/*diras1a:gfp* and *diras1b* MO/*diras1b:gfp* at 24 hpf. When five mismatched MOs

were co-injected into embryos with a *diras1*:*gfp* fusion gene, the GFP signal was detected in most injected embryos (Supplementary Fig. 2). To determine the function of *diras1* in neurodevelopment and to verify the functional redundancy of *diras1* among different species, we co-injected the *diras1a* and/or *diras1b* MOs with wild-type or truncated mouse *Diras1* mRNA into the *Tg(huC:gfp)* zebrafish to track the generation of terminally differentiated neurons. Off-target effects were avoided in this study by using specific MOs that were co-injected with twofold amounts of *p53* MO in all MO experiments. From the lateral view of the embryos, high levels of *huC* expression in the telencephalic cluster were found in the control and MO plus wild-type groups but not in the truncated mouse *Diras1* mRNA groups. *diras1a* and/or *diras1b* morphants exhibited abrogated *huC* expression in the forebrain region. Only a small number of *huC*-positive neurons were present in the *diras1a* and/or *diras1b* morphants unlike in the control and MO plus wild-type mouse *Diras1* mRNA groups (Fig. 6). Therefore, *diras1a* and/or *diras1b* knockdown in zebrafish embryos affects neuronal development. To confirm further that these events specifically resulted from the downregulation of *diras1*, we conducted acetylated α-tubulin (AcTub) staining to determine whether the disruption of *diras1a* and/or *diras1b* affects neuronal differentiation. At 24 hpf, AcTub staining revealed decreased axonal branching of trigeminal ganglion sensory neurons (TG) in morphants that received *diras1a* MO and/or *diras1b* MO. Co-injection with mouse *Diras1*, but not with *Diras1*-ct mRNA, recovered axonal branching. Moreover, the TG

clusters were smaller in *diras1a* and/or *diras1b* morphants compared with those in control morphants (Fig. 7A). Given the defect in TG observed through AcTub staining, we investigated whether *diras1a* and *diras1b* contribute to trigeminal ganglion development during embryogenesis by analyzing the expression of islet1/2. Anti-islet1/2 staining, which highlights the differentiated trigeminal neurons at 24 hpf, indicates that the TG was well-developed in control MO-injected embryos. By contrast, the disruption of either *diras1a* or *diras1b* exhibited a gross number of development defects resulting from the loss of TG (Fig. 7B). The trigeminal ganglion neurons were 28.8 ± 2.3, 21.4 ± 2.1, and 18.7 ± 2.9 in the control, *diras1a* morphants, and *diras1b* morphants, respectively. However, the co-knockdown of *diras1a* and *diras1b* had no synergistic effects on trigeminal ganglion neurons, which were reduced to a 17.1 ± 3.2 level. Interestingly, co-injection with wild-type, but not with the C-terminus truncated form of mouse *Diras1* mRNA, restored the neurons of trigeminal ganglion to 29 ± 2.1 (Fig. 7C). Moreover, we injected splice morpholino (Sp-MO) into embryos and found that *diras1*-Sp-MO morphants display similar defects as ATG-MO (Supplementary Figs. 3 and 4). This result implies that *diras1a* and *diras1b* may be necessary for the proper development of trigeminal ganglions. A recent study has shown that the first TGs are born as individuals at 11 hpf and are widely scattered along the anterior-posterior axis lateral to the midbrain and the midbrain-hindbrain boundary. Meanwhile, the anterior TGs then migrate, condense with the posterior neurons, and rapidly aggregate into compact

clusters to reach the site of ganglion assembly at 14 hpf [34]. This process raises the question of whether the disruptions of *diras1a* and *diras1b* alter the motility of initial trigeminal cells from the anterior to the posterior. As shown in Fig. 8A, the early development of trigeminal precursors is determined by the expression of *ngn1*, and these precursors are initially widely scattered in the control embryos at 11 hpf. Thereafter, the precursors converge into a coherent ganglion at 14 hpf, as monitored by *neuroD* expression (Fig. 8B). The knockdown of either *diras1a* or *diras1b* did not alter the development of the initial precursors and the assembly of trigeminal ganglions as confirmed by the lack of overt alternation of *ngn1* and *neuroD* expression (Figs. 8A and B). Aspreviously mentioned, *diras1a*- and *diras1b*-mediated neuronal differentiation depend onRac1 activity. Thus, in the next set of experiments, we investigate whether the constitutive activation of Rac1 can repair TG defects in *diras1* morphants. Indeed, co-injection with mRNA derived from constitutively active human *Rac1* restored the neurons of the trigeminal ganglion to the level of the control group (Figs. 9A and B). Our results reveal that the *diras1* gene may contribute to the maintenance of the number of trigeminal ganglions through the Rac1-dependent pathway.

Discussion

The activation of the Ras superfamily of proteins can regulate a wide range of biological functions, such as cell proliferation, cell invasion, cell migration, differentiation, and

apoptosis [9,35]. In this work, we demonstrated the expression and conducted a functional analysis of zebrafish *diras1* genes. Both *diras1a* and *diras1b*, two human *DIRAS1* homologues, were mainly expressed in the central nervous system and in the dorsal neuron ganglions with distinct and overlapping patterns. The overexpression of the wild types, but not of CAAX motif-truncated forms of *diras1a* and *diras1b*, triggered lamellipodia-like morphology and facilitated neurite outgrowth in Neuro-2a cells by modulating Rac1 and RhoA. Blocking Rac1 signals through dominant negative Rac1, Pak1, or CDK5, as well as Arp2/3 inhibition significantly reduced these phenomena in *diras1a*- and *diras1b*-expressing cells. The interference of *diras1a* and/or *diras1b* markedly reduced the cell population of trigeminal ganglions. Co-injection with mouse *Diras1* mRNA or constitutively active *Rac1* mRNA clearly restored the trigeminal ganglion population. Our collective findings reveal that *diras1* genes serve a pivotal role in neuronal function through the Rac1-dependent pathway.

Finely orchestrated actin reorganization serves a pivotal role in neuron functions, such as specification, polarization, axon guidance, and migration [36]. Accumulated evidence reveals that the Rho subfamily, specifically Rac1, CDC42, and RhoA, serves an indispensable function in neuronal cytoskeleton reorganization. In one study, in response to extracellular or intracellular cues, CDC42 and Rac1 triggered filopodia and lamillepodia, respectively, which both resulted in neurite outgrowth. By contrast, RhoA stimulated stress fiber formation and caused the collapse of neurites [37]. The stimulation of rat pheochrocytoma PC12 cells with

nerve growth factor (NGF) or serum starvation of mouse neuroblastoma N1E-115 cells reportedly caused neurite formation by upregulating Rac1 and CDC42 activities but was retarded by the dominant negative forms of Rac1 and CDC42 [38,39]. In another study, blocking Rac1 affected the axon growth of the Drosophila neuron [40]. Forced expression of the constitutively activated form of Rac1 facilitated the neurite outgrowth in rat hippocampal neurons [41]. By contrast, inhibition of RhoA by dominant negative RhoA or by RhoA inhibitor resulted in neurite outgrowth in mouse neural stem cells [42], whereas constitutively active RhoA attenuated the neurite outgrowth induced by NGF, BDNF, and neurotrophin 3 [43]. In line with these observations, our findings demonstrate that the wild-type, but not truncated forms, of *diras1* elevated the activities and protein level of Rac1, decreased the RhoA protein level, and subsequently triggered neuronal differentiation in Neuro-2a cells. Either the dominant negative Rac1 or the constitutively active RhoA blocked the *diras1*-induced neuronal polarization. Taken as a whole, our results suggest that *diras1* genes promote neuronal differentiation by modulating Rac1 and RhoA. However, the molecular mechanisms underlying the *diras1*-dependent reduction of RhoA remain under investigation.

Evidence indicates that Pak1 regulates neuronal dynamics [30]. GTP-bound active Rac1 interacts with the N-terminal region of Pak1, which stimulates Pak1 activity. This condition triggers cytoskeleton reorganization, which results in neurite outgrowth in neuronal cells [30]. The constitutively active Pak1 enhances neurite number, whereas the dominant negative

Pak1 attenuates neurite number in cortical neuron cells [44]. *Hayashi et al*. demonstrated that dominant negative Pak1 significantly decreased constitutively active Rac1-induced neurites in cultured pyramidal neurons [44]. In another study, *Tahirovic et al*. demonstrated that Pak1 activities were abolished in cerebella isolated from Rac1 knockout [33]. In line with these observations, we showed that dominant negative Pak1 reduced neuronal differentiation in *diras1a*- or *diras1b*-overexpressing Neuro-2a cells. Interestingly, no significant alternation of the phosphorylation of cofilin, a substrate of Pak1, was found in cells with and without *diras1* overexpression (data not shown). A previous report has shown that Rac2, but not Rac1, is involved in the dephosphorylation of cofilin in response to formyl-methionyl-leucyl-phenylalanine receptor activation [45]. Altogether, our data suggest that Pak1, but not cofilin activity, serves a crucial function in *diras1*-mediated actin cytoskeleton rearrangement.

CDK5 and its associated protein, p35, were shown to serve critical functions in the formation of neurite outgrowth during neuron differentiation [28]. CDK5/p35 also develops complex and active forms of Rac1 and can regulate actin cytoskeleton rearrangement [29]. Moreover, p35/CDK5/Rac1 complex was found to trigger actin cytoskeleton reorganization through hyperphosphorylation and Pak1 inhibition, eventually causing neurite outgrowth in cultured neuronal cells [29,46]. In this study, dominant negative CDK5 also blocked *diras1*-induced polarization in Neuro-2a cells. Our collective findings reveal that CDK5 is

involved in the *diras1*-mediated neuronal differentiation as a downstream target of Rac1.

Reports also show that the WAVE/Arp2/3 pathways are involved in the Rac1-mediated actin cytoskeleton reorganization [47]. The WAVE regulatory complex binds to the active Rac1 and activates Arp2/3, thus causing actin polymerization [47]. *Miki et al*. have shown that WAVE interactes with Rac1 in Cos7 cells for the co-expression of WAVE and Rac1 [48]. The dominant negative WAVE inhibits the Rac1-induced membrane ruffling but does not affect the CDC42-induced spike-like formation [33]. Mislocalization of the WAVE in the cytosolic region was observed in the cerebellar granule neurons of Rac1 knockout mice [33]. The forced expression of WAVE overcame the defects in neuron polarization caused by the Rac1 knockout [33]. In this study, the forced expression of *diras1a* or *diras1b* stimulated the WAVE level, but not the alternation of Arp2/3 expression. However, CK-458 blocked Arp2/3 activities and diminished *diras1a* and *diras1b*-induced neuronal polarization. Our collective results indicate that the WAVE/Arp2/3 pathways may also be involved in the *diras1*-induced actin reorganization in neuronal cells.

In this study, the knockdown of *diras1a* and/or *diras1b* decreased the number of the trigeminal ganglion in zebrafish. More interestingly, *Kanungo et al*. demonstrated that the depletion of CDK5 expression by si-RNA reduced the primary sensory neurons of the trigeminal ganglion in zebrafish [49]. Our results suggest that CDK5 may function as a downstream effector of *diras1* genes. Thus, the knockdown of *diras1a* and/or *diras1b* may

prevent CDK5 activity and subsequently decrease the trigeminal ganglion neurons. However, the overt alternation of the trigeminal ganglion precursor markers, such as *ngn1* and *neuroD*, was absent among the morphants and the control group at 11 hpf and 14 hpf, respectively. The lack of influence of *ngn1* and *neuroD* expressions in the early trigeminal ganglion of *diras1* morphants may be explained by the temporal expression patterns of *diras1a* and *diras1b*. The trigeminal ganglion precursor first appeared at 11 hpf as a small cluster of approximately 14 neurons, which reached 30 neurons at 24 hpf and consisted of approximately 55 neurons at 72 hpf [50]. *Caron et al*. showed that early-born and late-born trigeminal ganglions display distinct genes and functions [50]. However, *diras1a* and *diras1b* were rarely detectable before 12 hpf when using RT-PCR and whole mount *in situ* hybridization. This finding suggests that both *diras1a* and *diras1b* are not essential for early trigeminal ganglion migration but may serve a critical function in neuron population.

This study is the first to demonstrate that zebrafish *diras1a* and *diras1b* promote neurite outgrowth in Neuro-2a cells and maintain trigeminal ganglion neurons in zebrafish. Both *diras1a* and *diras1b* enhance Rac1 levels and downregulate the RhoA level. Blocking Rac1 downstream targets significantly prevents the effects of *diras1a*- and *diras1b*-induced polarization in Neuro-2a cells. The depletion of *diras1a* and *diras1b* results in decreased trigeminal ganglion neurons. Such decrease can be restored by co-injection of mouse *Diras1* or constitutively active *Rac1* mRNA. In conclusion, our findings indicate that *diras1a* and

diras1b are key factors in neurogenesis because of their cross-talks with other small GTPases, such as Rac1 and RhoA.

References

1. Colicelli J (2004) Human RAS superfamily proteins and related GTPases. Sci STKE 2004: RE13.
2. Mitin N, Rossman KL, Der CJ (2005) Signaling interplay in Ras superfamily function. Curr Biol 15: R563-574.
3. Wennerberg K, Rossman KL, Der CJ (2005) The Ras superfamily at a glance. J Cell Sci 118: 843-846.
4. Bourne HR, Sanders DA, McCormick F (1991) The GTPase superfamily: conserved structure and molecular mechanism. Nature 349: 117-127.
5. Ellis CA, Vos MD, Howell H, Vallecorsa T, Fults DW, et al. (2002) Rig is a novel Ras-related protein and potential neural tumor suppressor. Proc Natl Acad Sci U S A 99: 9876-9881.
6. Fukata M, Kaibuchi K (2001) Rho-family GTPases in cadherin-mediated cell-cell adhesion. Nat Rev Mol Cell Biol 2: 887-897.
7. Hall A (1998) Rho GTPases and the actin cytoskeleton. Science 279: 509-514.
8. Luo L (2000) Rho GTPases in neuronal morphogenesis. Nat Rev Neurosci 1: 173-180.
9. Ridley AJ, Paterson HF, Johnston CL, Diekmann D, Hall A (1992) The small GTP-binding protein rac regulates growth factor-induced membrane ruffling. Cell 70: 401-410.
10. Nobes CD, Hall A (1995) Rho, rac, and cdc42 GTPases regulate the assembly of multimolecular focal complexes associated with actin stress fibers, lamellipodia, and filopodia. Cell 81: 53-62.
11. Ridley AJ, Hall A (1992) The small GTP-binding protein rho regulates the assembly of focal adhesions and actin stress fibers in response to growth factors. Cell 70: 389-399.
12. Olenik C, Barth H, Just I, Aktories K, Meyer DK (1997) Gene expression of the small GTP-binding proteins RhoA, RhoB, Rac1, and Cdc42 in adult rat brain. Brain Res Mol Brain Res 52: 263-269.
13. Albertinazzi C, Gilardelli D, Paris S, Longhi R, de Curtis I (1998) Overexpression of a neural-specific rho family GTPase, cRac1B, selectively induces enhanced

neuritogenesis and neurite branching in primary neurons. J Cell Biol 142: 815-825.

14. Brown MD, Cornejo BJ, Kuhn TB, Bamburg JR (2000) Cdc42 stimulates neurite outgrowth and formation of growth cone filopodia and lamellipodia. J Neurobiol 43: 352-364.
15. Yamashita T, Tucker KL, Barde YA (1999) Neurotrophin binding to the p75 receptor modulates Rho activity and axonal outgrowth. Neuron 24: 585-593.
16. Kontani K, Tada M, Ogawa T, Okai T, Saito K, et al. (2002) Di-Ras, a distinct subgroup of ras family GTPases with unique biochemical properties. J Biol Chem 277: 41070-41078.
17. Tada M, Gengyo-Ando K, Kobayashi T, Fukuyama M, Mitani S, et al. (2012) Neuronally expressed Ras-family GTPase Di-Ras modulates synaptic activity in Caenorhabditis elegans. Genes Cells 17: 778-789.
18. Westerfield M, Doerry E, Kirkpatrick AE, Douglas SA (1999) Zebrafish informatics and the ZFIN database. Methods Cell Biol 60: 339-355.
19. Westerfield M, Doerry E, Kirkpatrick AE, Driever W, Douglas SA (1997) An on-line database for zebrafish development and genetics research. Semin Cell Dev Biol 8: 477-488.
20. Kimmel CB, Ballard WW, Kimmel SR, Ullmann B, Schilling TF (1995) Stages of embryonic development of the zebrafish. Dev Dyn 203: 253-310.
21. Thisse C, Thisse B (2008) High-resolution in situ hybridization to whole-mount zebrafish embryos. Nat Protoc 3: 59-69.
22. Hsu LS, Tseng CY (2010) Zebrafish calcium/calmodulin-dependent protein kinase II (cam-kii) inhibitors: expression patterns and their roles in zebrafish brain development. Dev Dyn 239: 3098-3105.
23. Hsu LS, Liang CJ, Tseng CY, Yeh CW, Tsai JN (2011) Zebrafish Cyclin-Dependent Protein Kinase–Like 1 (zcdkl1): Identification and Functional Characterization. Int J Mol Sci 12: 3606-3617.
24. Schmidt A, Hall A (2002) Guanine nucleotide exchange factors for Rho GTPases: turning on the switch. Genes Dev 16: 1587-1609.
25. Auer M, Hausott B, Klimaschewski L (2011) Rho GTPases as regulators of morphological neuroplasticity. Ann Anat 193: 259-266.
26. Manser E, Chong C, Zhao ZS, Leung T, Michael G, et al. (1995) Molecular cloning of a new member of the p21-Cdc42/Rac-activated kinase (PAK) family. J Biol Chem 270: 25070-25078.
27. Bokoch GM (2003) Biology of the p21-activated kinases. Annu Rev Biochem 72: 743-781.
28. Kesavapany S, Li BS, Pant HC (2003) Cyclin-dependent kinase 5 in

neurofilament function and regulation. Neurosignals 12: 252-264.
29. Nikolic M, Chou MM, Lu W, Mayer BJ, Tsai LH (1998) The p35/Cdk5 kinase is a neuron-specific Rac effector that inhibits Pak1 activity. Nature 395: 194-198.
30. Kreis P, Barnier JV (2009) PAK signalling in neuronal physiology. Cell Signal 21: 384-393.
31. Pollard TD, Borisy GG (2003) Cellular motility driven by assembly and disassembly of actin filaments. Cell 112: 453-465.
32. Stradal TE, Scita G (2006) Protein complexes regulating Arp2/3-mediated actin assembly. Curr Opin Cell Biol 18: 4-10.
33. Tahirovic S, Hellal F, Neukirchen D, Hindges R, Garvalov BK, et al. (2010) Rac1 regulates neuronal polarization through the WAVE complex. J Neurosci 30: 6930-6943.
34. Knaut H, Blader P, Strahle U, Schier AF (2005) Assembly of trigeminal sensory ganglia by chemokine signaling. Neuron 47: 653-666.
35. Oxford G, Theodorescu D (2003) Ras superfamily monomeric G proteins in carcinoma cell motility. Cancer Lett 189: 117-128.
36. Cheever TR, Ervasti JM (2013) Actin isoforms in neuronal development and function. Int Rev Cell Mol Biol 301: 157-213.
37. Govek EE, Newey SE, Van Aelst L (2005) The role of the Rho GTPases in neuronal development. Genes Dev 19: 1-49.
38. Aoki K, Nakamura T, Matsuda M (2004) Spatio-temporal regulation of Rac1 and Cdc42 activity during nerve growth factor-induced neurite outgrowth in PC12 cells. J Biol Chem 279: 713-719.
39. Sarner S, Kozma R, Ahmed S, Lim L (2000) Phosphatidylinositol 3-kinase, Cdc42, and Rac1 act downstream of Ras in integrin-dependent neurite outgrowth in N1E-115 neuroblastoma cells. Mol Cell Biol 20: 158-172.
40. Luo L, Liao YJ, Jan LY, Jan YN (1994) Distinct morphogenetic functions of similar small GTPases: Drosophila Drac1 is involved in axonal outgrowth and myoblast fusion. Genes Dev 8: 1787-1802.
41. Schwamborn JC, Puschel AW (2004) The sequential activity of the GTPases Rap1B and Cdc42 determines neuronal polarity. Nat Neurosci 7: 923-929.
42. Gu H, Yu SP, Gutekunst CA, Gross RE, Wei L (2013) Inhibition of the Rho signaling pathway improves neurite outgrowth and neuronal differentiation of mouse neural stem cells. Int J Physiol Pathophysiol Pharmacol 5: 11-20.
43. Da Silva JS, Medina M, Zuliani C, Di Nardo A, Witke W, et al. (2003) RhoA/ROCK regulation of neuritogenesis via profilin IIa-mediated control of actin stability. J Cell Biol 162: 1267-1279.
44. Hayashi K, Ohshima T, Hashimoto M, Mikoshiba K (2007) Pak1 regulates

dendritic branching and spine formation. Dev Neurobiol 67: 655-669.
45. Sun CX, Magalhaes MA, Glogauer M (2007) Rac1 and Rac2 differentially regulate actin free barbed end formation downstream of the fMLP receptor. J Cell Biol 179: 239-245.
46. Rashid T, Banerjee M, Nikolic M (2001) Phosphorylation of Pak1 by the p35/Cdk5 kinase affects neuronal morphology. J Biol Chem 276: 49043-49052.
47. Takenawa T, Miki H (2001) WASP and WAVE family proteins: key molecules for rapid rearrangement of cortical actin filaments and cell movement. J Cell Sci 114: 1801-1809.
48. Miki H, Suetsugu S, Takenawa T (1998) WAVE, a novel WASP-family protein involved in actin reorganization induced by Rac. EMBO J 17: 6932-6941.
49. Kanungo J, Li BS, Goswami M, Zheng YL, Ramchandran R, et al. (2007) Cloning and characterization of zebrafish (Danio rerio) cyclin-dependent kinase 5. Neurosci Lett 412: 233-238.
50. Caron SJ, Prober D, Choy M, Schier AF (2008) In vivo birthdating by BAPTISM reveals that trigeminal sensory neuron diversity depends on early neurogenesis. Development 135: 3259-3269.

Acknowledgements

These authors thank Dr. Yi-Shuian Huang (Institute of Biomedical Sciences, Academia Sinica, Taipei, Taiwan) for provided pCMV-mCherry plasmid and Addgene for provided plasmids as mentioned in “Material and methods” section. This study was supported by grants obtained from the Ministry of Science and Technology of Taiwan (MOST-103-2311-B-040-001). The authors thank the Zebrafish Core in Academia Sinica (ZCAS), Institute of Cellular and Organismic Biology (ICOB), which is supported by grant NSC-103-2321-B-001-050 from the National Science Council (NSC), the Taiwan Zebrafish Core Facility (TZCF) for providing the zebrafish AB strain and *Tg*(*huc:gfp*), and the National Health Research Institute (NHRI), which is supported by grant 100-2321-B-400-003 from National Science Council (NSC).

Upright fluorescent microscopy was performed in the Instrument Center of Chung Shan Medical University, which is supported by the National Science Council, Ministry of Education and Chung Shan Medical University.

Conflicts of Interest These authors declare that there are no conflicts of interest.

FIGURE LEGENDS

Fig. 1. Protein sequence alignments, phylogenetic tree and expression patterns of zebrafish *diras1a* and *diras1b*. (a) Multiple alignments of *diras1a* and *diras1b* amino acid sequences were compared with those of human (*H-DI-Ras1*), mouse (*M-DI-Ras1*), rat (*R-DI-Ras1*), and *Xenopus* (*X-DI-Ras1*). The *DIRAS1* sequences from the five species were aligned using ClustalW. Identical sequences are shaded in yellow, whereas residue similarities of the four *DIRAS1* proteins are presented in cyan. (b) A phylogenetic tree was constructed based on the multiple alignments of the DIRAS1 proteins using MegAlign in DNASTAR through the neighbor joining method. Scale bars indicate nucleotide substitutions (100×). (c) A graphical representation of the conserved synteny of the *DIRAS1* gene clusters in human chromosome 19, rat chromosome 7, mouse chromosome 10, and zebrafish linking groups (LG) 2. The *diras1a* gene is localized in LG 11. Ch denotes the chromosome. Whole mount *in situ* hybridization was performed using antisense riboprobes against *diras1a* (d) and *diras1b* (e) at the indicated

developmental stages. The stages of embryonic development are indicated in the right (d,e). di: diencephalon, GCL: ganglion cell layer, H.B.: hindbrain, and tel: telencephalon. Stages are indicated in the upper right.

Fig. 2. Zebrafish *diras1* enhanced neurite outgrowth in Neuro-2a cells. (a,b) Neuro-2a cells were transiently transfected with pEGFP vectors, namely, pEGFP-*diras1a*, pEGFP-*diras1b*, pEGFP-*diras1a*-ct, or pEGFP-*diras1b*-ct. The cells were fixed at 24 h post-transfection, and the actin cytoskeleton was stained with rhodamine/phalloidin (in red) (a) to determine the percentage of cells with neurite outgrowth. The *arrowhead* indicates lamellipodia-like structure. The *arrow* indicates protrusion formation. (b). *Scale bars* (a): 50 μm. The nucleus was stained with DAPI (in blue). Data are presented as the mean ± S.D. of three independent experiments. ***$p < 0.001$ (Student's *t* test).

Fig. 3. Functional characterization of zabrafish *diras1a* and *diras1b*. (a) Neuro-2a cells were transfected with pEGFP vectors, namely, pEGFP-*diras1a*, pEGFP-*diras1b*, pEGFP-*diras1a*-ct, or pEGFP-*diras1b*-ct. The protein levels of Rac1, Cdc42, and RhoA were detected using Western blot analysis. β-Actin was used for normalization. (b) Data are presented as the mean ± S.D. of three independent experiments. *$p < 0.05$; **$p < 0.01$. (c) Rac1 activity was assessed by extracting GTP-bound Rac1 proteins from cell lysates using the GST-Pak1-PBD fusion protein. About 500 μg of lysates derived from cells transfected with the indicated plasmids were incubated with GST-Pak1-PBD or GST alone. After the pull-down assay, Rac1

was detected with immunoblotting. Whole input lysate was detected with an anti-GFP antibody. Coomassie blue-stained SDS-PAGE gels show the molecular weight of the GST and the GST-Pak1-PBD fusion protein.

Fig. 4. Rac1 inactivation, RhoA activation, Pak1 inhibition, or CDK5 inhibition blocked *diras1*-induced neurite outgrowth. (a,b) Neuro-2a cells were co-transfected with pEGFP-*diras1a* or pEGFP-*diras1b* combined with pYFP vector or pYFP-dominant negative Rac1 (T17N). The cells were fixed and stained with rhodamine/phalloidin (in red) at 24 h post-transfection to examine the percentage of neuronal cell differentiation (b). Neuro-2a cells were co-transfected with pEGFP-*diras1a* or pEGFP-*diras1b* combined with pCMV-mCherry vector or pCMV-mCherry-constitutive activated RhoA (Q63L), pCMV-mCherry-catalytically inactivated Pak1 (K299R) or pCMV-mCherry-dominant negative CDK5 (D145N) for 24 h. The cells were fixed, and the neurite outgrowth rate was examined. Images show the morphology of the cells (c). The panel shows the percentages of cell differentiation (d). *Scale bars* (a,c): 50 μm. The nucleus was stained with DAPI (in blue). Data are presented as the mean ± S.D. of three independent experiments. ***$p < 0.001$ (Student's *t* test).

Fig. 5. WAVE and Arp2/3 were involved in *diras1*-mediated neurite outgrowth. (a) Neuro-2a cells were transfected with pEGFP vectors, namely, pEGFP-*diras1a*, pEGFP-*diras1b*, pEGFP-*diras1a*-ct, or pEGFP-*diras1b*-ct. The protein levels of WAVE and Arp2/3 were detected using Western blot analysis. β-Actin was used for normalization. (b) Data are

presented as the mean ± S.D. of three independent experiments. (c,d) Neuro-2a cells with or without pre-treatment with Arp2/3 inhibitor (CK-548) were transfected with pEGFP vectors, namely, pEGFP-*diras1a* or pEGFP-*diras1b*. The cells were fixed and stained with rhodamine/phalloidin (in red) at 24 h post-transfection to investigate morphological changes. The nucleus was stained with DAPI (in blue). *Scale bars* (c): 50 μm. Data are presented as the mean ± S.D. of three independent experiments. ***$p < 0.001$ (Student's *t* test).

Fig. 6. Effects of *diras1* gene depletion on neurogenesis using the *Tg*(*huC*:*gfp*) model. The embryos that received the indicated MOs were collected at 48 hpf. The expression of *huC* was abrogated in *diras1* morphants. Reduced trigeminal sensory ganglion territories were also observed in *diras1* morphants. The deficiency in *huC* expression was restored via co-injection with the wild-type but not with the C-terminus truncated form of mouse *Diras1 m*RNA. All images are shown in lateral view. *Scale bars*: 100 μm. Tc: telencephalic cluster, Tg: trigeminal ganglion, Tec: tectum, and Hb: hindbrain.

Fig. 7. Effects of *diras1* depletion on neurogenesis as visualized using acetylated tubulin (AcTub) and islet1/2 staining. (a) AcTub expression (an axonal marker) was examined using confocal microscopy at 24 hpf. The axonal scaffolds of the trigeminal sensory ganglion in *diras1* morphants were visibly curtailed. Co-injection with the wild-type but not with the C-terminus truncated form of mouse *Diras1* mRNA restored the neurons of the trigeminal ganglion. The *arrowhead* indicates the trigeminal sensory ganglion. (b) Embryos that

received the indicated MO were collected at 24 hpf. The trigeminal sensory ganglion was marked using an islet1/2 antibody via immunostaining. Trigeminal sensory ganglia decreased in *diras1a* and *diras1b* morphants. These defects can be restored by mouse *Diras1* mRNA. All images are shown in lateral view. *Scale bars*: 100 μm. (c) Data are presented as the mean ± S.D. of three independent experiments. *$p < 0.05$, the morphant group compared with the control MO; #$p < 0.05$, co-injection with the wild-type mRNA group compared with the morphant group (Student's *t* test). *Scale bars* (a,b): 100 μm.

Fig. 8. Knockdown of *diras1* did not impair the positioning of the trigeminal sensory ganglion. (a,b) The embryos that received the indicated MO with or without the corresponding RNA were collected. Whole mount *in situ* hybridization for *ngn1* expression at 11 hpf (a) and *neuroD* expression at 14 hpf (b) was performed. Trigeminal sensory ganglia were settled in small clusters at 11 hpf and formed compact clusters at 14 hpf. This arrangement is indistinguishable between the control and morphants. Precursors of the trigeminal sensory ganglion (tg) are indicated. All images are in dorsal view with the anterior at the top. *Scale bars* (a,b): 100 μm.

Fig. 9. Zebrafish *diras1* was required for trigeminal sensory gangliongenesis through the Rac1-dependent pathway. (a) The morphants that received the indicated MOs were collected at 24 hpf. An islet1/2 antibody was used as a marker of the trigeminal sensory ganglion. Trigeminal sensory ganglia decreased in *diras1a* or/and *diras1b* morphants. These defects can

be restored by injecting the constitutive activation of *Rac1* mRNA. All images are shown in lateral view. *Scale bars* (a): 100 μm. (b) Quantitative analyses of islet1/2-positive neurons are presented as the mean ± S.D. of three independent experiments. *$p < 0.05$, the morphant group compared with the control MO; #$p < 0.05$, co-injection with the wild-type mRNA group compared with the morphant group (Student's *t* test).

Fig. S1. Neuro-2a cells were transfected with inhibitory constructs alone and did not cause morphological change. Neuro-2a cells were transiently transfected with various inhibitory constructs. Data are presented as the mean ± S.D. of three independent experiments.

Fig. S2. Specificity of *diras1a* and *diras1b* morpholinos. Two GFP reporter plasmids (*diras1a:gfp* and *diras1b:gfp*) that encompass the MO target sequences were constructed. Embryos that received 100 pg of *diras1a:gfp* or *diras1b:gfp* showed a mosaic GFP expression at 24 hpf. Co-injection of *diras1a:gfp* or *diras1b:gfp* with the corresponding MO but not the five-mismatched MOs significantly diminished GFP expression. *Scale bars*: 1 mm.

Fig. S3. Zebrafish *diras1a* and *diras1b* splice morpholino (Sp-MO) effectively blocked the correct splicing of pre-mRNA without compensation effects. (a) Schematic indicates the intron and exon structures and position of Sp-MO (red) and RT-PCR primers (arrows). (b) Embryos were injected at the single-cell stage with *diras1a* and/or *diras1b* Sp-MO. RNAs were extracted and analyzed using RT-PCR. Corrected splicing fragments were found in the control MO groups but not in the *diras1a* and/or *diras1b* Sp-MO groups. Lane 1: marker, lane

2: control MO, lane 3: control MO, lane 4: *diras1a*-Sp-MO, lane 5: *diras1b*-Sp-MO, lane 6: *diras1a*- and *diras1b*-Sp-MO. (c) RT-PCR analyses of the *diras1a* and *diras1b* gene in *diras1* morphants suggested that the knockdown of *diras1a* or *diras1b* did not induce the complementary effect. Lane 1: marker, lane 2: control MO, lane 3: *diras1a*-Sp-MO, lane 4: control MO, lane 5: *diras1b*-Sp-MO. Elongation factor 1α was used as the internal control.

Fig. S4. Loss of the trigeminal ganglion in *diras1a* and/or *diras1b* Sp-MO morphants. (a) The embryos that received the indicated Sp-MO were collected at 24 hpf. The trigeminal sensory ganglion was marked using an islet1/2 antibody via immunostaining. All images are shown in lateral view. *Scale bars*: 100 μm. (b) Quantitative analyses of islet1/2-positive neurons are presented as the mean ± S.D. of three independent experiments. *$p < 0.05$, the morphant group compared with the control MO (Student's *t* test).

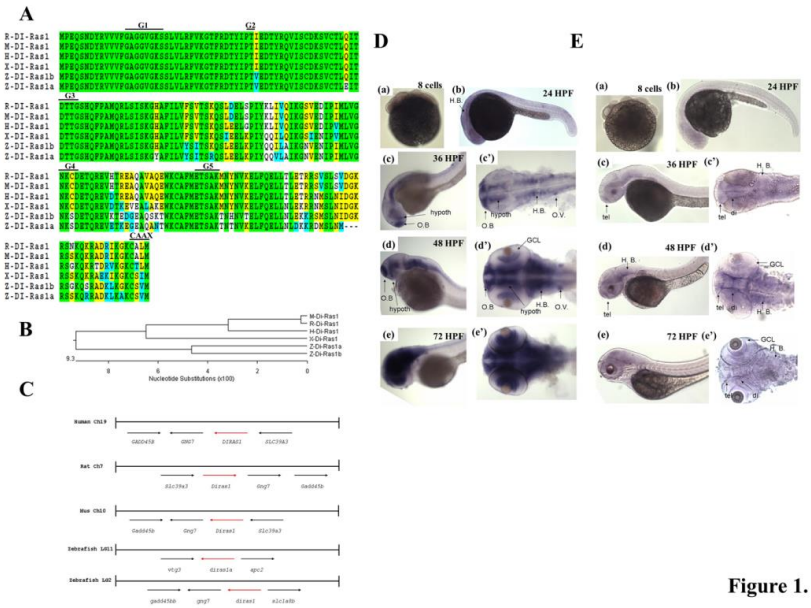
A
G1
G2
G3
G4
G5
CAAX
R-DI-Ras1
M-DI-Ras1
H-DI-Ras1
X-DI-Ras1
Z-DI-Ras1b
Z-DI-Ras1a
B
M-DI-Ras1
R-DI-Ras1
H-DI-Ras1
X-DI-Ras1
Z-DI-Ras1a
Z-DI-Ras1b
9.3
8
6
4
2
0
Nucleotide Substitutions (x100)
C
Human Chr9
Rat Chr7
Mus Chr6
Zebrafish LG11
Zebrafish LG2
D
E
8 cells
24 HPF
36 HPF
48 HPF
72 HPF
hypoth
H. B.
O. B
O. V.
GCL
tel

Figure 1.

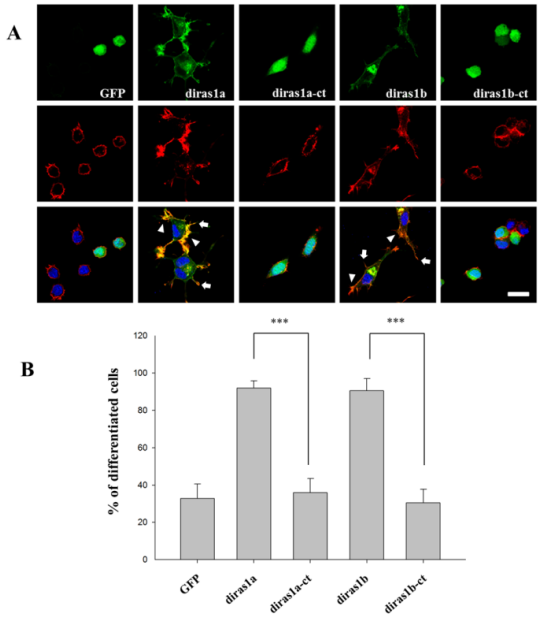
A
GFP
diras1a
diras1a-ct
diras1b
diras1b-ct
B
% of differentiated cells
120
100
80
60
40
20
0
***
***
GFP
diras1a
diras1a-ct
diras1b
diras1b-ct

Figure 2.

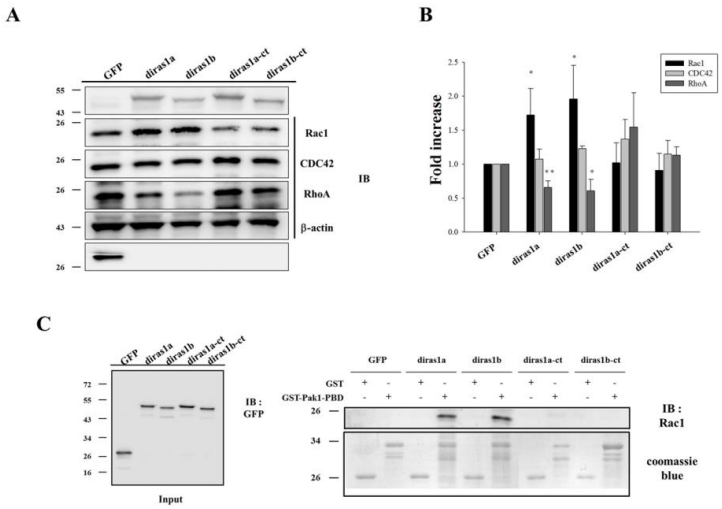
A
GFP
diras1a
diras1b
diras1a-ct
diras1b-ct
55
43
26
Rac1
CDC42
RhoA
β-actin
IB
B
Rac1
CDC42
RhoA
Fold increase
2.5
2.0
1.5
1.0
0.5
0.0
GFP
diras1a
diras1b
diras1a-ct
diras1b-ct
C
GFP
diras1a
diras1b
diras1a-ct
diras1b-ct
72
55
43
34
26
16
IB :
GFP
Input
GST
GST-Pak1-PBD
IB :
Rac1
coomassie
blue

Figure 3.

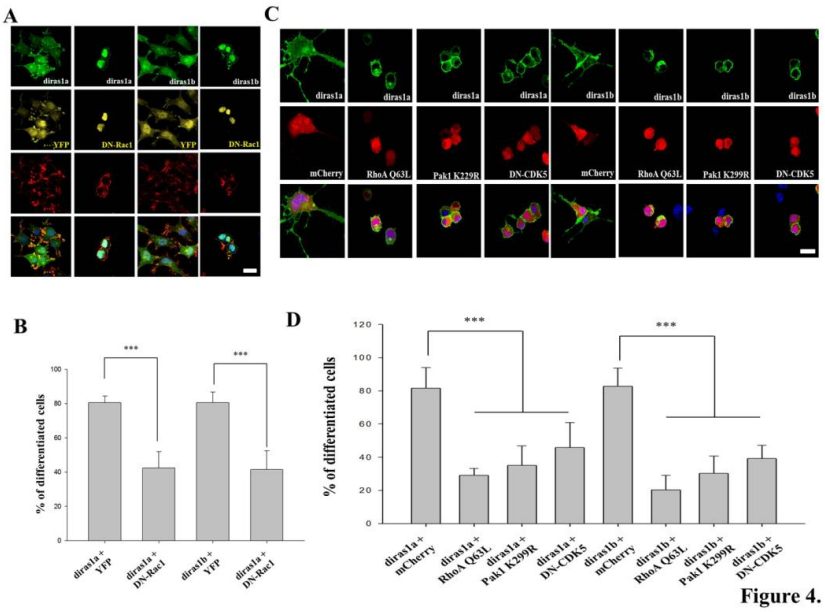
A
diras1a
diras1a
diras1b
diras1b
YFP
DN-Rac1
YFP
DN-Rac1
C
diras1a
diras1a
diras1a
diras1a
diras1b
diras1b
diras1b
diras1b
mCherry
RhoA Q63L
Pak1 K299R
DN-CDK5
mCherry
RhoA Q63L
Pak1 K299R
DN-CDK5
B
% of differentiated cells
***
***
dras1a + YFP
dras1a + DN-Rac1
dras1b + YFP
dras1a + DN-Rac1
D
% of differentiated cells
***
***
dras1a + mCherry
dras1a + RhoA Q63L
dras1a + Pak1 K299R
dras1a + DN-CDK5
dras1b + mCherry
dras1b + RhoA Q63L
dras1b + Pak1 K299R
dras1b + DN-CDK5

Figure 4.

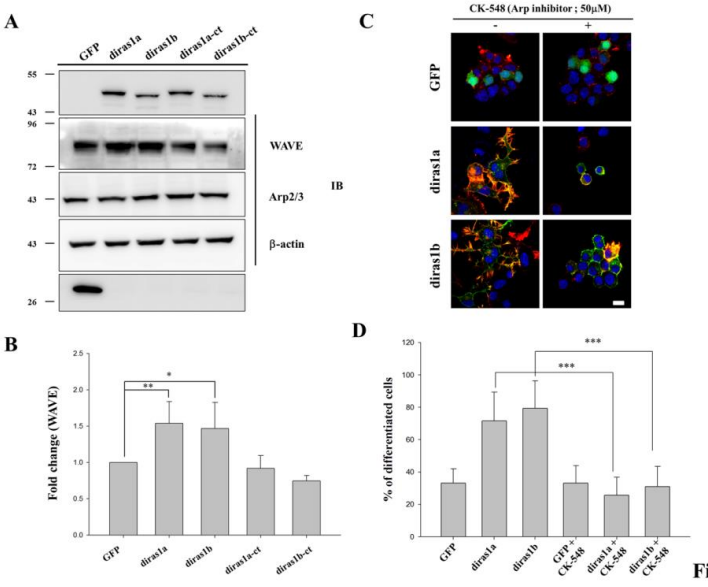
A
GFP
dIras1a
dIras1b
dIras1a-ct
dIras1b-ct
55
43
96
72
43
43
26
WAVE
Arp2/3
β-actin
IB
B
Fold change (WAVE)
2.5
2.0
1.5
1.0
0.5
0.0
*
**
GFP
dIras1a
dIras1b
dIras1a-ct
dIras1b-ct
C
CK-548 (Arp inhibitor ; 50μM)
-
+
GFP
dIras1a
dIras1b
D
% of differentiated cells
120
100
80
60
40
20
0
***
***
GFP
dIras1a
dIras1b
GFP + CK-548
dIras1a + CK-548
dIras1b + CK-548

Figure 5.

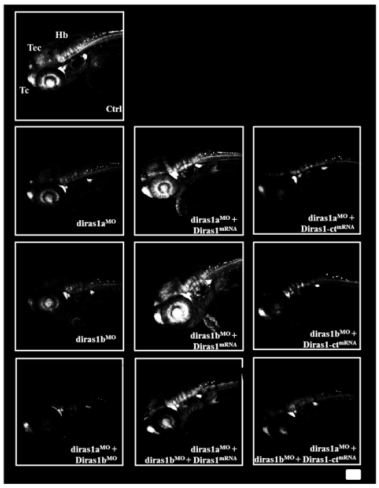
Hb
Tec
Tc
Ctrl
diras1a^MO
diras1a^MO + Diras1^mRNA
diras1a^MO + Diras1-ct^mRNA
diras1b^MO
diras1b^MO + Diras1^mRNA
diras1b^MO + Diras1-ct^mRNA
diras1a^MO + Diras1b^MO
diras1a^MO + diras1b^MO + Diras1^mRNA
diras1a^MO + diras1b^MO + Diras1-ct^mRNA

Figure 6.

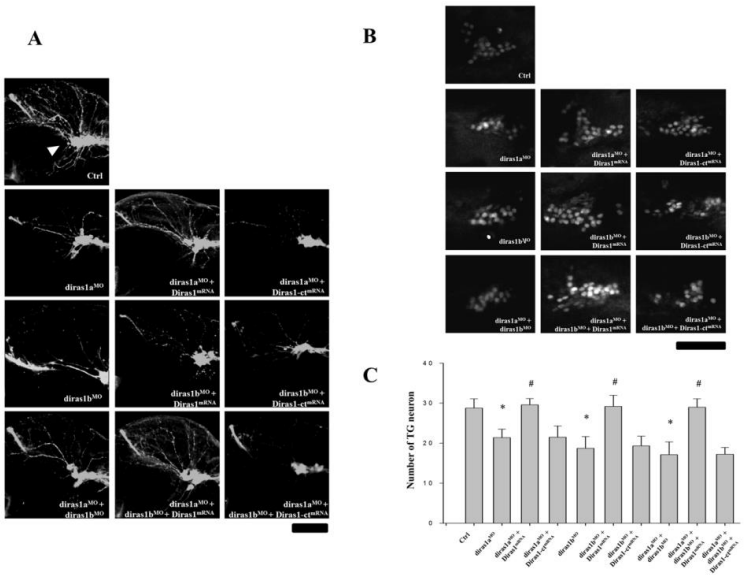
A
Ctrl
diras1a^MO
diras1a^MO + Diras1^mRNA
diras1a^MO + Diras1-ct^mRNA
diras1b^MO
diras1b^MO + Diras1^mRNA
diras1b^MO + Diras1-ct^mRNA
diras1a^MO + diras1b^MO
diras1a^MO + diras1b^MO + Diras1^mRNA
diras1a^MO + diras1b^MO + Diras1-ct^mRNA
B
Ctrl
diras1a^MO
diras1a^MO + Diras1^mRNA
diras1a^MO + Diras1-ct^mRNA
diras1b^MO
diras1b^MO + Diras1^mRNA
diras1b^MO + Diras1-ct^mRNA
diras1a^MO + diras1b^MO
diras1a^MO + diras1b^MO + Diras1^mRNA
diras1a^MO + diras1b^MO + Diras1-ct^mRNA
C
Number of TG neuron
0
10
20
30
40
*
#

Figure 7.

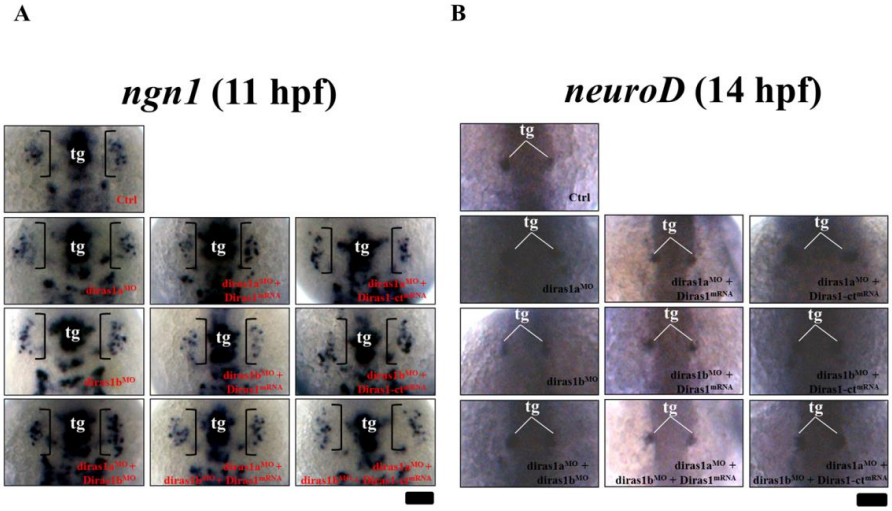
A
B
ngn1 (11 hpf)
neuroD (14 hpf)
tg
Ctrl
dias1a^MO
dias1a^MO + Dias1^mRNA
dias1a^MO + Dias1-ct^mRNA
dias1b^MO
dias1b^MO + Dias1^mRNA
dias1b^MO + Dias1-ct^mRNA
dias1a^MO + dias1b^MO
dias1a^MO + dias1b^MO + Dias1^mRNA
dias1a^MO + dias1b^MO + Dias1-ct^mRNA

Figure 8.

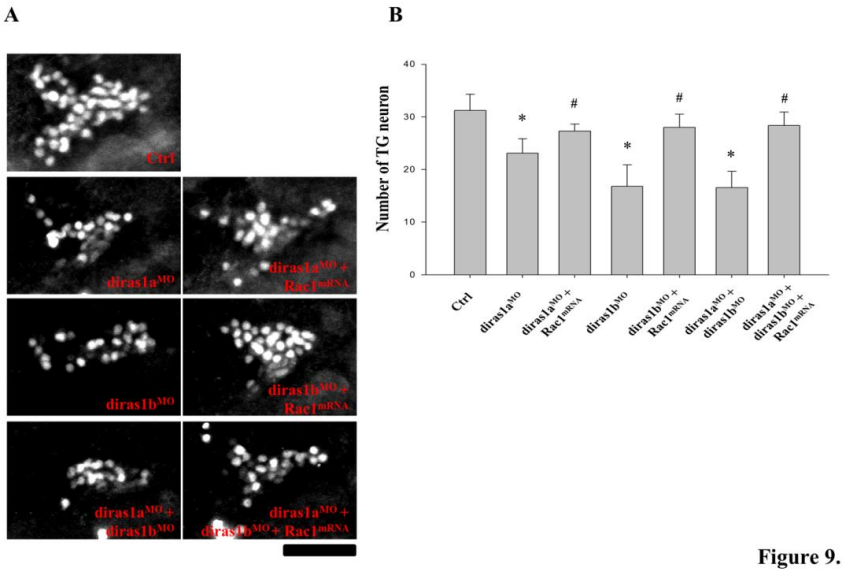
A
B
Ctrl
diras1a^MO
diras1a^MO + Rac1^mRNA
diras1b^MO
diras1b^MO + Rac1^mRNA
diras1a^MO + diras1b^MO
diras1a^MO + diras1b^MO + Rac1^mRNA
Number of TG neuron
0
10
20
30
40
*
#

Figure 9.

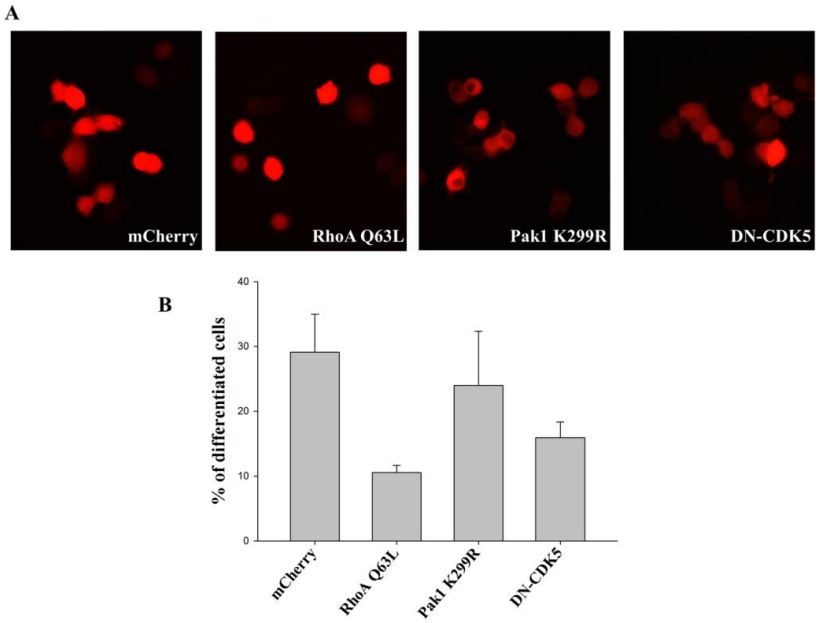
A
mCherry
RhoA Q63L
Pak1 K299R
DN-CDK5
B
% of differentiated cells
40
30
20
10
0
mCherry
RhoA Q63L
Pak1 K299R
DN-CDK5

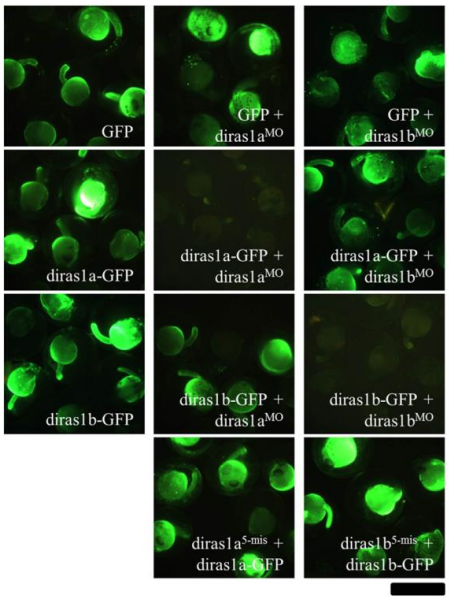
GFP
GFP +
diras1a^MO
GFP +
diras1b^MO
diras1a-GFP
diras1a-GFP +
diras1a^MO
diras1a-GFP +
diras1b^MO
diras1b-GFP
diras1b-GFP +
diras1a^MO
diras1b-GFP +
diras1b^MO
diras1a^5-mis +
diras1a-GFP
diras1b^5-mis +
diras1b-GFP

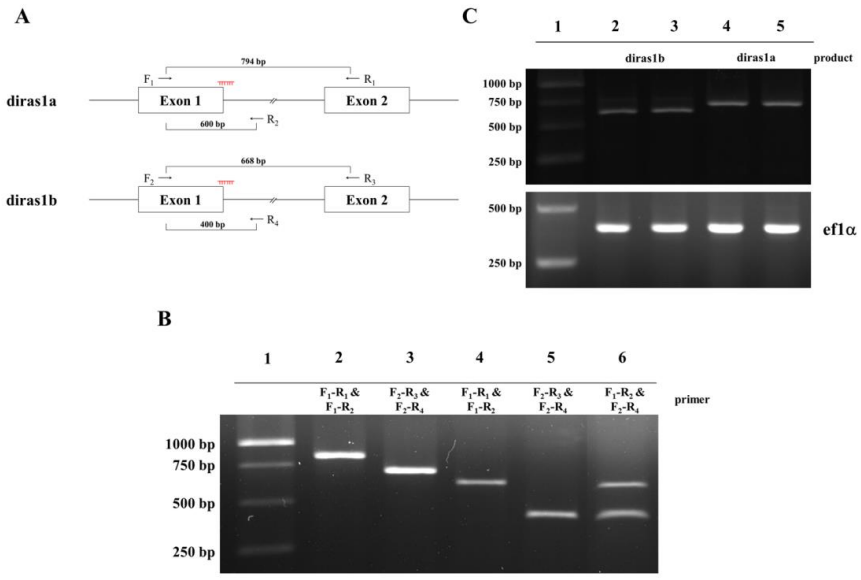
A
diras1a
794 bp
F1
R1
Exon 1
Exon 2
600 bp
R2
diras1b
668 bp
F2
R3
Exon 1
Exon 2
400 bp
R4
C
1 2 3 4 5
diras1b
diras1a
product
1000 bp
750 bp
500 bp
250 bp
500 bp
250 bp
ef1α
B
1 2 3 4 5 6
F1-R1 & F1-R2
F2-R3 & F2-R4
F1-R1 & F1-R2
F2-R3 & F2-R4
F1-R2 & F2-R4
primer
1000 bp
750 bp
500 bp
250 bp

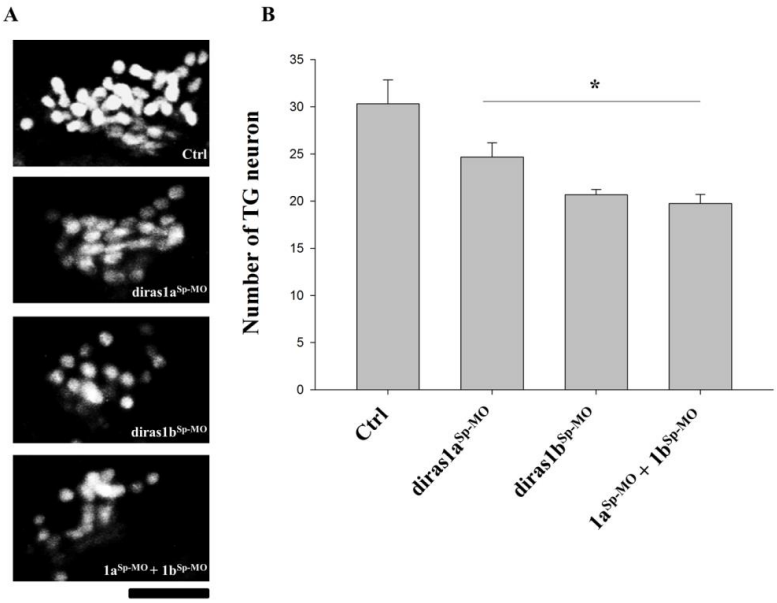
A
B
Ctrl
diras1a Sp-MO
diras1b Sp-MO
1a Sp-MO + 1b Sp-MO
Number of TG neuron
35
30
25
20
15
10
5
0
*
Ctrl
diras1a Sp-MO
diras1b Sp-MO
1a Sp-MO + 1b Sp-MO

附件五

國科會補助專題研究計畫出席國際學術會議心得報告

日期：103 年 11 月 12 日

計畫編號	MOST 103-2311-B-040 -001 -		
計畫名稱	探討斑馬魚 di-ras 基因及其相關基因在神經發育所扮演的角色		
出國人員 姓名	許立松	服務機構 及職稱	中山醫學大學 生物化學研究所 教授
會議時間	104 年 06 月 2 日 至 104 年 06 月 05 日	會議地點	日本筑波
會議名稱	(中文) 第四十八屆 日本發生生物學會大會 (英文) **48th** Japan Society of Developmental Biologists		
發表題目	(中文) 斑馬魚中 diras1a 及 diras1b 的表現模式以及功能分析 (英文) **Expression patterns and functional characterization of zebrafish di-ras1a anddi-ras1b**		

一、參加會議經過

於 6 月 1 日晚抵達東京，6 月 2 日搭乘筑波快線到達筑波並領取大會手冊。6 月 4 日晚上 5 點至 6 點於展出海報處說明研究成果。海報展示期間，多位學者表示對本研究的高度興趣，並有多方討論。

二、與會心得

此次會議由日本發育生物學會主辦，在 plenary 演講主要是由從 Oxford 大學來的 Holland 博士演講 gene duplication 在 homeobox 基因上所扮演的特殊角色，由於目前所研究的基因在斑馬魚中亦有

gene duplication 現象，且此兩個 duplicated gene 表現模式不一樣但是在斑馬魚胚胎發育過程中似乎都參與了 trigeminal ganglion 的發育，聽完此演講給我許多的啟示包含 gene duplication 後雖然造成不同基因的表現但是由於是同一個基因所分裂而來，因此可能有相同的作用。另一個 plenary 演講是由 Mukouyama 博士主講，他所提的有關於神經-肌肉的訊息傳遞之間的關聯性，在心臟發育過程中，心臟的平滑肌肌肉會分泌神經生長分子(NGF)一方面可以促使神經突觸產生，而非先形成心臟再藉由神經生長去產生突觸。另外也去聽斑馬魚的神經發育有關聯的幾場演講。Meuller 博士所講的有關於斑馬魚的前腦發育中細胞生長因子所扮演的角色，Kawatami 博士利用 Gal4-UAS 方式去探討斑馬魚端腦的各結構的不同功能，這次許多的國內年輕學者研究也被選為口頭報告，也引起不少回響，參加此次會議讓我可以跟國內外一些學者互相溝通學習，收穫不少。

三、發表論文全文或摘要

Abstract

The small GTPase Ras superfamily regulates several neuronal functions including neurite outgrowth and neuron proliferation. In this study, zebrafish *diras1a* and *diras1b* were identified and were found to be mainly expressed in the central nervous system and dorsal neuron ganglion. Overexpression of GFP-*diras1a* or GFP-*diras1b* triggered neurite outgrowth of Neuro-2a cells. The wild types, but not the C-terminus truncated forms, of *diras1a* and *diras1b* elevated the protein level of Rac1 and downregulated RhoA expression. GST pull-down assay also revealed that *diras1a* and *diras1b* enhanced Rac1 activity. Interfering with Rac1, Pak1, or CDK5 activity or with the Arp2/3 inhibitor prevented *diras1a* and *diras1b* from mediating the neurite outgrowth effects. In the zebrafish model, knockdown of *diras1a* and/or *diras1b* by morpholino antisense oligonucleotides not only reduced axon guidance but also caused the loss of trigeminal ganglion without affecting the precursor markers, such as *ngn1* and *neuroD*. Co-injection with mRNA derived from mouse *Diras1* or constitutively active human *Rac1* restored the population of trigeminal ganglion. In conclusion, we provided preliminary evidence that *diras1* is involved in neurite outgrowth and maintains the number of trigeminal ganglions through the Rac1-dependent pathway.

Keyword: diras1, neurite outgrowth, rac1, trigeminal ganglion, zebrafish

Introduction

The Ras GTPase superfamily proteins function as important regulators in a wide variety of biological processes, including proliferation, differentiation, signal transduction, protein synthesis, and cell metabolism [1-3]. The Ras superfamily is divided into five subfamilies according to their sequence homology and biochemical properties. The five families are Ras, Rho, Rab, Ran, and Arf [3]. The Ras superfamily switches between two states, namely, a GTP-bound active form and a GDP-bound inactive form. The activation of Ras proteins is mediated by guanine nucleotide exchange factors that facilitate the exchange of the GDP-bound form and is deactivated by GTPase-activating proteins that enhance intrinsic GTP hydrolysis. When bound to GTP, Ras proteins associate with effectors, which results in the propagation of downstream signaling [4,5].

Recent evidence suggests that Rho subfamily proteins are key regulators of the actin cytoskeleton, cell adhesion [6,7], and cell polarization [8]. The most understood proteins in the Rho-family GTPase are Ras-related C3 botulinum toxin

substrate 1 (Rac1), cell division cycle 42 (cdc42), and Ras homologous member A (RhoA). Rac1 induces lamellipodium formation through actin polymerization, Cdc42 regulates the formation of filopodia [9,10], and RhoA mediates stress fiber formation [11]. These three Rho family GTPases, which may be involved in neuron development, are predominantly expressed throughout the nervous system in such areas as the hippocampus, cerebellum, thalamus, and neocortex [12]. Emerging reports indicate that Rho GTPases regulate the axonal initiation and motility of neurite terminals. Rac1 and Cdc42 generally serve as positive regulators that promote neurite growth [13,14], whereas RhoA activation appears to serve as a negative regulator that suppresses neurite growth [15].

Ellis et al. and *Kontoni et al*. recently identified novel Ras members, namely, DIRAS1 and DIRAS2 proteins, which belong to a distinct subfamily of Ras GTPases [5,16]. The mRNA transcripts of *DIRAS1* and *DIRAS2* are specifically expressed in adult human brain tissues [5,16]. DIRAS1 and DIRAS2 exhibit low levels of intrinsic nucleotide hydrolysis activity and predominantly exist in a GTP-bound state [16]. The forced expression of *DIRAS1* does not affect Raf kinase and thus fails to trigger MAPK activation and Elk-1 transactivation [5,16]. DIRAS1 has been described as a potential tumor suppressor that attenuates the growth of human glioblastomas [5]. Recent evidence from the *Caenorhabditis elegans* model suggests that *drn-1*, a *DIRAS1* homologue in *C. elegans*, is restricted in neuron cells and is required for neuromuscular junctions [17].

Although *drn-1* has been shown to modulate synaptic activity in motor neurons [17], the biological function of DIRAS1 in neuron development remains uncertain. In this study, we perform functional analysis and provide evidence of the expression patterns of two zebrafish *diras1* genes: *diras1a* and *diras1b*. Both genes are predominantly expressed in the brain region and retina ganglion cells. The ectopic expression of the wild-type, but not the C-terminus truncated form, of *diras1* genes in Neuro-2a cells induces protrusion formation. Zebrafish *diras1a* and *diras1b* are found to elevate the protein level and activities of Rac1 and attenuate RhoA expression in Neuro-2a cells. Blocking Rac1 downstream signals abrogates *diras1a*- and *diras1b*-induced neurite outgrowth. Interfering with *diras1a* and/or *diras1b* expression decreases the number of trigeminal ganglia. Co-injection of the wild-type, but not the C-terminal truncated form, of mouse *Diras1* mRNA and constitutively active *Rac1* mRNA rescues the MO-induced effects. Altogether, these data comprise the preliminary evidence highlighting the function of diras1 proteins in neuronal development.

Materials and Method

Ethics statement

All procedures involving experimental animals described in this work were approved by the Institutional Animal Care and Use Committee (IACUC Approval NO. 1344) of Chung-Shan Medical University Experimental Animal Center.

Fish maintenance

Zebrafish (*Danio rerio*) AB strains and transgenic *Tg*(*huC:gfp*) fish were provided by the Taiwan Zebrafish Core Facility (Academia Sinica, Taiwan). The fish were kept at 28 ℃ under standard conditions [18,19]. The developmental stages of the fish were determined according to the morphological criteria described by Kimmel et al. [20].

Reagents

All chemicals were purchased from Sigma Chemical Company or J. T. Baker. Antibodies against GFP, Pak1, RhoA, Rac1, CDC42, WAVE, and Arp2/3 were purchased from Santa Cruz Biotechnology. Anti-β-actin and horseradish

peroxidase (HRP)-conjugated secondary antibodies were obtained from Sigma Chemicals Company. Fetal bovine serum and penicillin–streptomycin mixture were obtained from Gibco Laboratory. Plasmids, namely, DN-Rac1 (Plasmid #20151), pcDNA3-EGFP-RhoA-Q63L (Plasmid #12968), pCMV6M-Pak1-K299R (Plasmid #12210), CDK5-DN-HA (Plasmid #1873) and pGEX-Pak1 83-149 (Plasmid #12216) were purchased from Addgene.

Isolation of zebrafish cDNAs

Total RNAs derived from the different stages were purified using TRIzol Reagent (Invitrogen) according to manufacturer's recommendations. Total RNA (5 μg) and a random primer were used for the synthesis of first-strand cDNA with MMLV reverse transcriptase (Promega). PCR amplification was performed using 1 μl of cDNA as the template and the following specific primers: wild-type zebrafish *diras1a*, 5′-GCAGCATGCCAGAGCAGAG-3′ (sense) and 5′-GGCAGCATACAAATCATGAC-3′ (anti-sense: R_1); wild-type zebrafish *diras1b*, 5′-GATGCCTGAGCAGAGCAACG-3′ (sense) and 5′-GCAAGTCTACATGACACTGC-3′ (anti-sense: R_3); C-terminal truncate zebrafish *diras1a*, 5′-CTACTTGGCCTTCAGCTTGTC-3′ (anti-sense); C-terminal truncate zebrafish *diras1b*, 5′-TCATTTCCCCTTCAGCTTGTC-3′ (anti-sense); wild-type mouse *diras1*, 5′-ATGCCAGAACAGAGCAATGAC-3′ (sense) and 5′-GGGCTCACATGAGCGCGCAC-3′ (anti-sense); and C-terminal truncate mouse *diras1*, 5′-TCACTTGCCCTTGATGCGGTCAG-3′ (anti-sense). PCR was programmed as follows: denaturation at 95 ℃ for 5 min followed by 35 cycles of 94 ℃ for 30 s, 55 ℃ for 30 s, and 72 ℃ for 1 min. The final extension was at 72 ℃ for 5 min. The negative control was concomitantly prepared using water instead of cDNA. The amplification of elongation factor 1α was used as the loading control. Amplified fragments were subcloned into the pGEM-T easy and $pCS2^+$.

Morpholino oligonucleotides and mRNA injections

All morpholino antisense oligonucleotides were designed and synthesized by Gene Tools, LLC (Philomath, OR): *diras1a* MO: (5'-GGTAATCGTTACTCTGCTCTGGCAT-3'); *diras1b* MO: (5'-AGTCGTTGCTCTGCTCAGGCATCTT-3'); *diras1a*-5mis MO: (5'-GCTAATCCTTAGTCTCCTCTCGCAT-3'); *diras1b*-5mis MO: (5'-AGTCCTTCCTCTCCTCACGGATCTT-3'); *diras1a* splice MO: (5'-AAAGCGATGTATTCTTACCTGGCGA-3'); *diras1b* splice MO: (5'-ACGTTCTAGACCTAGTAGAGAGAAA-3'); *p53* MO: (5'-GCGCCATTGCTTTGCAAGAATTG-3'); control MO: (5'-CCTCTTACCTCAGTTACAATTTATA-3') corresponding to the human β-globin gene was used as a negative control. MOs were dissolved in 1x Danieau solution and injected into the embryos at the one- to two-cell stage. Efficiencies of splice morpholinos were confirmed by PCR on cDNA derived from morpholino-injected embryos using the following primers: diras1a splice forward (Exon: F_1), 5'-TTTGGGACGTTGCAACACAG-3'; diras1a splice reverse (Intron: R_2), 5'-GGAATGCAGATATGAGATGGC-3'; diras1b splice forward (Exon: F_2), 5'-GATCAGTCACGCGGGACACG-3'; diras1b splice reverse (Intron: R_4), 5'-AAGCGGCTCTCTGTAATCGG-3'.

In situ hybridization

The entire coding sequences and partial 3′-untranslated regions of *diras1a* and *diras1b* were amplified and subcloned into the pGEM-T easy vector (Promega, USA). The digoxigenin-labeled anti-sense riboprobes for both genes were synthesized through *in vitro* transcription by SP6 RNA polymerase following the manufacturer's standard protocol (Roche, Swiss). Whole mount *in situ* hybridization was performed as previously described [21].

Cell culture, transfection, and differentiation of neuroblastoma cells

Mouse neuroblastoma Neuro-2a cells (BCRC 60026) were purchased from Bioresource Collection and Research Center and stored in MEM supplemented with 10% fetal bovine serum, 100 μg/ml of streptomycin and 100 U/ml of penicillin. The cells were kept in a humidified 5% CO_2 incubator. Plasmid DNA was transfected into Neuro-2a cells using Lipofectamine reagent (Invitrogen, USA). The cell lysates were collected 24 h post-transfection. Morphological changes were assessed. Six to seven areas were randomly photographed from three independent experiments via LSM META 510 confocal microscopy (Zeiss). The results were compared using Student's *t*-test.

GST-pull down assay

The GST and GST-Pak1 (amino acid residues 83-149) were expressed in DH5α bacterial cells and purified according to standard procedures, as previously described [22]. The cell lysates from overexpressed cells indicated that plasmids were obtained, and protein concentrations were measured using a Bradford protein assay kit (Bio-Rad). Cell lysates (500 μg) were incubated with 5 μg of GST or GST-Pak1 (amino acids residues 83-149) fusion protein overnight at 4 ℃. After washing thrice with lysis buffer, the complexes were subjected to Western blot analysis using the specific antibody against Rac1 to determine the activated form of Rac1.

Western blot analysis

The cell lysates derived from *diras1a*- or *diras1b*-overexpressing cells were obtained. Protein (50 μg) was separated using 10% polyacrylamide gel and then transferred into nitrocellulose membranes. The membrane was blocked with phosphate-buffered saline (PBS) containing 5% nonfat milk for 1 h at room temperature. Thereafter, the membrane was probed with the indicated primary antibodies at 4 ℃ overnight. The membrane was washed with PBS containing 0.1% Tween-20 (PBST) and then reacted with HRP-conjugated secondary antibody (Santa Cruz Biotechnology). The membrane was again extensively washed with PBST, after which the reactive signal was detected using an enhanced chemiluminescence kit (Amersham Pharmacia Biotech, UK). The β-actin expression was used as the internal control.

Immunostaining

Briefly, embryos at the indicated stages were collected, fixed in 4% paraformaldehyde at 4 ℃ overnight, and then stored in methanol at −20 ℃. After rehydration with PBST (PBS containing 0.1% Tween 20), the embryos were blocked with blocking solution (5% goat serum, 2% bovine serum albumin, and 1% DMSO in PBST) for 1 h and then incubated with primary antibodies at 4 ℃ overnight. Samples were washed with PBST and incubated with secondary antibodies in blocking buffer at 4 ℃ overnight in the dark. After washing with buffer solution (2% BSA and 1% DMSO in PBST), images were captured using a scanning laser confocal microscope (510 META ZEISS). The primary antibodies include mouse anti-acetylated α-tubulin (1:1000) and rabbit anti-isl1/2 (1:200). The secondary antibodies include goat anti-mouse conjugate-FITC (1:500) and goat anti-rabbit Alexa Fluor 568 (1:500).

Results

Zebrafish *diras1a* and *diras1b* are predominantly expressed in the brain region

In previous experiments, we performed microarray analysis and identified the downstream targets of zebrafish regulator of g-protein signaling 7 (rgs7) gene, namely, calcium/calmodulin-dependent protein kinase II (cam-kii) inhibitors and cyclin-dependent protein kinase–like 1 (zcdkl1) [22,23]. In this study, we selected another putative rgs7 target (GenBank Accession No. NM-199831.1) for further investigation. The *diras1a* gene contains 2142 base pairs and encodes a polypeptide of 195 amino acid residues. In a BLASTP search of diras1a amino

acids, one gene (LOC565395; GenBank Accession No.NM-001126421.1), which is highly similar to human *DIRAS1*, was found and designated as *diras1b*. The 198 amino acids encoded a diras1b protein and shared 90% identity and 95% similarity with diras1a. The homologies of the deduced amino acid sequences of diras1 and those of other species were analyzed using the CLUSTALW program (Fig. 1A). diras1a and diras1b showed amino acid alignments similar to those from rats, mice, and humans (ranging from 80% to 87%). Motif research of the diras1 sequences showed that they contain a well-conserved guanine-nucleotide-binding domain. The G1 domain contains the GXXXXGKS motif (corresponding to Residues 14 to 21 of both genes). The invariant T of the G2 domain and the DXXG motif of G3 domain were found in Residue 39 and Residues 61 to 64, respectively. The conserved motifs NKXD in the G4 domain and EXSAK in the G5 domain were localized in Residues 121 to 124 and 148 to 152, respectively. In addition, both diras1a and diras1b contained the C-terminal CAAX (A represents aliphatic or aromatic amino acids, whereas X represents amino acid residue is critical for determine the type of covalent isoprenylation) motif, with X being a methionine. This finding suggests that both genes are putative substrates for farnesyl transferase. Based on the phylogenetic analysis, zebrafish *diras1a* and *diras1b* are members of a separate cluster (Fig. 1B). To determine whether *diras1a* and *diras1b* genes share a conserved synteny with mammalian species, we compared the gene order around *diras1a* and *diras1b* in zebrafish, humans, rats, and mice. The *diras1b* gene clustered with growth arrest and DNA-damage–induced beta (*gadd45bb*), guanine nucleotide binding protein gamma 7 (*gng7*), and silute carrier protein family 1, member 8b (*slc1a8b*). During linking, group 2 exhibited conserved synteny with the genes in human Chromosome 19, rat Chromosome 7, and mouse Chromosome 10 (Fig. 1C). *diras1a* was flanked by *adenomatous polyposis coli 2* (*apc2*) and *vitellogenin 3* (*vtg3)*. Our results suggest that *diras1b* is a true orthologue of mammalian *DIRAS1*, whereas *diras1a* is generated from whole genome duplication. Whole mount *in situ* hybridization analysis revealed that no RNA transcripts of *diras1a* and *diras1b* were found at the 32-cell stage. At 24 h post-fertilization (hpf), *diras1a* RNA was diffusedly expressed in the brain region with high expression in the hindbrain region. By contrast, *diras1b* was weakly expressed in the brain region. At 36 hpf, *diras1a* was abundantly expressed in the olfactory bulb, ventral rostral cluster of the ventral telencephalon, hypothalamus, hindbrain, otic vesicle, and neurons in the dorsal spinal cord. At 48 hpf, *diras1a* expression was strong in the olfactory bulb, thalamus, diencephalons, otic vesicle, and midbrain, as well as in the ganglion cell layer (GCL) of the retina. Low levels of *diras1a* were also found in dorsal spinal cord neurons. At 72 hpf, *diras1a* expression was enhanced throughout the whole brain region, as well as in the GCL and inner nuclear layer of the retina (Fig. 1D). By contrast, the transcript of *diras1b* was weakly expressed in the telencephalon, diencephalon, and hindbrain at 36 hpf. At 48 hpf and 72 hpf, *diras1b* appeared in the telencephalon, diencephalon, hindbrain, and GCL of the retina (Fig. 1E).

Zebrafish *diras1a* and *diras1b* promote neurite outgrowth in Neuro-2a cells

Given that zebrafish *diras1a* and *diras1b* were specifically expressed in the neuron system, we used mouse neuroblastoma cell line Neuro-2a, which is widely employed to study the mechanisms of neuronal differentiation, as an *in vitro* model to investigate the biological function of *diras1a* and *diras1b*. Neuro-2a cells were transfected with various GFP-tagged forms of *diras1*. At 24 h post-transfection, GFP-*diras1a* and GFP-*diras1b* were found to be localized to the plasma membrane region. By contrast, a lone GFP vector was widely expressed in whole cells. The truncated mutant GFP-*diras1a*-ct or GFP-*diras1b*-ct, which lacks the CAAX terminal membrane-anchoring motif, was also expressed diffusedly in the cells. Interestingly, Neuro-2a cells transfected with GFP-*diras1a* or GFP-*diras1b* exhibited lamellipodia-like morphological changes, as evidenced by F-actin staining (Fig. 2A). Lamellipodia-like formation is rarely observed among Neuro-2a cells with overexpressed GFP alone or in truncated mutant forms.

Quantitative analysis showed that the percentage of differentiation in GFP-*diras1a*- or GFP-*diras1b*-overexpressing cells was significantly higher than that in the control groups and that C-terminal truncated form-overexpressing mutants had no effect on differentiation (Fig. 2B). Therefore, zebrafish *diras1a* and *diras1b* may promote neurite outgrowth among Neuro-2a cells.

Functions of Rac1 and RhoA in the *diras1*-induced neurite outgrowth of Neuro-2a cells

Among the signaling molecules that control cell polarity, the Rho-family small GTPases (e.g., Rac1, Cdc42, and RhoA) are characterized by their functions in regulating cytoskeletal remodeling [8,24]. To evaluate which Rho GTPases are affected by *diras1a* and *diras1b*, we assessed the protein level using Western blot analysis. As shown in Figs. 3A and B, overexpression of GFP-*diras1a* and GFP-*diras1b* significantly increased Rac1 protein level and decreased RhoA protein expression, unlike the case of the truncated forms and control groups. However, a lack of alternation in Cdc42 expression was observed. Rac1 can reportedly induce neuronal polarization, whereas RhoA serves a critical function in collapsing the growth cone by promoting membrane retraction [25]. To elucidate further the functions of Rac1 and RhoA in *diras1*-induced neurite outgrowth, the dominant negative form of Rac1 (T17N) and constitutively activated RhoA (Q63L) were separately co-transfected with GFP-*diras1* into Neuro-2a cells. As expected, the cells with either decreased Rac1 activity or increased RhoA activity exhibited abrogated *diras1*-mediated neurite outgrowth morphology (Fig. 4A-D). Our results suggest that upregulation of Rac1 and downregulation of RhoA may be involved in *diras1*-induced neurite outgrowth. The activated GTP-bound form of Rac1/Cdc42 binds to the p21-binding domain (PBD) and subsequently increases Pak1 activities by interrupting the trans-inhibition of Pak1 [26,27]. To ascertain whether *diras1a* and *diras1b* enhances Rac1 activity, Rac1 activation status was assessed by extracting GTP-bound Rac1 proteins from cell lysates using a GST-PBD of Pak1 (amino acids residues 83-149) fusion protein. As shown in Fig. 3C, Rac1 is clearly present in lysates derived from cells that expressed GFP-*diras1a* and GFP-*diras1b*. By contrast, cells that expressed C-terminal truncated mutants relatively decreased their association with Pak1 (Fig. 3C). These results indicate that diras1-mediated neurite outgrowth can be attributed not only to the enhanced expression but also to the increased activities of Rac1.

Zebrafish *diras1* triggers neurite outgrowth by modulating Rac1 downstream effectors

Pak1 and CDK5 have recently been implicated in neuronal cytoskeleton dynamics [28]. Both Pak1 and CDK5 are the main kinases for Rac1-mediated normal neuronal differentiation and function [29,30]. We hypothesize that Pak1 and CDK5 contribute to diras1 signaling. To test this hypothesis, the kinase-inactive dominant negative CDK5 mutant (pCMV-Mcherry-Cdk5-D145N) or the catalytically inactive form of Pak1 (pCMV-Mcherry-Pak1-K299R) was co-transfected with GFP vector alone, GFP-*diras1a*, or GFP-*diras1b* into Neuro-2a cells. The expression of kinase-negative CDK5-D145N or Pak1-K299R significantly decreased protrusion in *diras1*-overexpressing Neuro-2a cells (Figs. 4C and D). Similarly, Neuro-2a cells was transfected with inhibitory constructs alone also presence the similar pattern compare to mCherry vector alone (Supplementary Fig. 1). Accumulated evidence suggests that Rac1 relays signaling cascades to the neuronal cytoskeleton using the Wiskott-Aldrich syndrome protein (WASP) family and the verprolin-homologous protein (WAVE) family, activates actin-related protein 2/3 (Arp2/3) complex-dependent nucleation, and subsequently provides a filamentous resource to organize actin polymerization [31-33]. To validate the functions of WAVE1 and Arp2/3 in *diras1*-induced polarization, Western blot analysis was conducted. As shown in Figs. 5A and B, wild types of *diras1a* and *diras1b* obviously elevated WAVE1 expression, unlike the deleted forms of *diras1a* and *diras1b* and GFP alone. However, no overt alternation of Arp2/3 expression was found. To determine whether

Arp2/3 affects *diras1*-induced polarization, an Arp2/3 inhibitor was used. The *diras1*-induced polarization phenotype was significantly blocked in Neuro-2a cells pre-treated with Arp2/3 inhibitor CK-548 (Figs. 5C and D). Accordingly, our findings imply that *diras1* triggers nuerite outgrowth using the Rac1 downstream effectors.

Depletion of *diras1a* and/or *diras1b* affects neural development in zebrafish

To address the function of *diras1* in zebrafish embryogenesis, we injected antisense MOs bounded to the ATG site and blocked the translation to one-cell stage embryos to knock down *diras1a*, *diras1b*, or both. To evaluate the specificity and effectiveness of *diras1a* MO and *diras1b* MO, *diras1a*:*gfp* and *diras1b:gfp* constructs, which are composed of morpholino target sequences fused to sequences encoding GFP, were generated and co-injected with the corresponding *diras1* MO. In addition, five mismatched MOs were used as negative controls. The expression of *diras1*:*gfp* was detected in the injected embryos at 24 hpf without developmental malformation. The GFP signal was diminished in embryos injected with *diras1a* MO/*diras1a:gfp* and *diras1b* MO/*diras1b:gfp* at 24 hpf. When five mismatched MOs were co-injected into embryos with a *diras1*:*gfp* fusion gene, the GFP signal was detected in most injected embryos (Supplementary Fig. 2). To determine the function of *diras1* in neurodevelopment and to verify the functional redundancy of *diras1* among different species, we co-injected the *diras1a* and/or *diras1b* MOs with wild-type or truncated mouse *Diras1* mRNA into the *Tg(huC:gfp)* zebrafish to track the generation of terminally differentiated neurons. Off-target effects were avoided in this study by using specific MOs that were co-injected with twofold amounts of *p53* MO in all MO experiments. From the lateral view of the embryos, high levels of *huC* expression in the telencephalic cluster were found in the control and MO plus wild-type groups but not in the truncated mouse *Diras1* mRNA groups. *diras1a* and/or *diras1b* morphants exhibited abrogated *huC* expression in the forebrain region. Only a small number of *huC*-positive neurons were present in the *diras1a* and/or *diras1b* morphants unlike in the control and MO plus wild-type mouse *Diras1* mRNA groups (Fig. 6). Therefore, *diras1a* and/or *diras1b* knockdown in zebrafish embryos affects neuronal development. To confirm further that these events specifically resulted from the downregulation of *diras1*, we conducted acetylated α-tubulin (AcTub) staining to determine whether the disruption of *diras1a* and/or *diras1b* affects neuronal differentiation. At 24 hpf, AcTub staining revealed decreased axonal branching of trigeminal ganglion sensory neurons (TG) in morphants that received *diras1a* MO and/or *diras1b* MO. Co-injection with mouse *Diras1*, but not with *Diras1*-ct mRNA, recovered axonal branching. Moreover, the TG clusters were smaller in *diras1a* and/or *diras1b* morphants compared with those in control morphants (Fig. 7A). Given the defect in TG observed through AcTub staining, we investigated whether *diras1a* and *diras1b* contribute to trigeminal ganglion development during embryogenesis by analyzing the expression of islet1/2. Anti-islet1/2 staining, which highlights the differentiated trigeminal neurons at 24 hpf, indicates that the TG was well-developed in control MO-injected embryos. By contrast, the disruption of either *diras1a* or *diras1b* exhibited a gross number of development defects resulting from the loss of TG (Fig. 7B). The trigeminal ganglion neurons were 28.8 ± 2.3, 21.4 ± 2.1, and 18.7 ± 2.9 in the control, *diras1a* morphants, and *diras1b* morphants, respectively. However, the co-knockdown of *diras1a* and *diras1b* had no synergistic effects on trigeminal ganglion neurons, which were reduced to a 17.1 ± 3.2 level. Interestingly, co-injection with wild-type, but not with the C-terminus truncated form of mouse *Diras1* mRNA, restored the neurons of trigeminal ganglion to 29 ± 2.1 (Fig. 7C). Moreover, we injected splice morpholino (Sp-MO) into embryos and found that *diras1*-Sp-MO morphants display similar defects as ATG-MO (Supplementary Figs. 3 and 4). This result implies that *diras1a* and *diras1b* may be necessary for the proper development of trigeminal ganglions. A recent study has shown that the first TGs are born as individuals at 11 hpf and are widely scattered along the anterior-posterior axis lateral to the midbrain and the midbrain-hindbrain boundary. Meanwhile, the anterior TGs then migrate, condense with the posterior

neurons, and rapidly aggregate into compact clusters to reach the site of ganglion assembly at 14 hpf [34]. This process raises the question of whether the disruptions of *diras1a* and *diras1b* alter the motility of initial trigeminal cells from the anterior to the posterior. As shown in Fig. 8A, the early development of trigeminal precursors is determined by the expression of *ngn1*, and these precursors are initially widely scattered in the control embryos at 11 hpf. Thereafter, the precursors converge into a coherent ganglion at 14 hpf, as monitored by *neuroD* expression (Fig. 8B). The knockdown of either *diras1a* or *diras1b* did not alter the development of the initial precursors and the assembly of trigeminal ganglions as confirmed by the lack of overt alternation of *ngn1* and *neuroD* expression (Figs. 8A and B). Aspreviously mentioned, *diras1a*- and *diras1b*-mediated neuronal differentiation depend onRac1 activity. Thus, in the next set of experiments, we investigate whether the constitutive activation of Rac1 can repair TG defects in *diras1* morphants. Indeed, co-injection with mRNA derived from constitutively active human *Rac1* restored the neurons of the trigeminal ganglion to the level of the control group (Figs. 9A and B). Our results reveal that the *diras1* gene may contribute to the maintenance of the number of trigeminal ganglions through the Rac1-dependent pathway.

Discussion

The activation of the Ras superfamily of proteins can regulate a wide range of biological functions, such as cell proliferation, cell invasion, cell migration, differentiation, and apoptosis [9,35]. In this work, we demonstrated the expression and conducted a functional analysis of zebrafish *diras1* genes. Both *diras1a* and *diras1b*, two human *DIRAS1* homologues, were mainly expressed in the central nervous system and in the dorsal neuron ganglions with distinct and overlapping patterns. The overexpression of the wild types, but not of CAAX motif-truncated forms of *diras1a* and *diras1b*, triggered lamellipodia-like morphology and facilitated neurite outgrowth in Neuro-2a cells by modulating Rac1 and RhoA. Blocking Rac1 signals through dominant negative Rac1, Pak1, or CDK5, as well as Arp2/3 inhibition significantly reduced these phenomena in *diras1a*- and *diras1b*-expressing cells. The interference of *diras1a* and/or *diras1b* markedly reduced the cell population of trigeminal ganglions. Co-injection with mouse *Diras1* mRNA or constitutively active *Rac1* mRNA clearly restored the trigeminal ganglion population. Our collective findings reveal that *diras1* genes serve a pivotal role in neuronal function through the Rac1-dependent pathway.

Finely orchestrated actin reorganization serves a pivotal role in neuron functions, such as specification, polarization, axon guidance, and migration [36]. Accumulated evidence reveals that the Rho subfamily, specifically Rac1, CDC42, and RhoA, serves an indispensable function in neuronal cytoskeleton reorganization. In one study, in response to extracellular or intracellular cues, CDC42 and Rac1 triggered filopodia and lamillepodia, respectively, which both resulted in neurite outgrowth. By contrast, RhoA stimulated stress fiber formation and caused the collapse of neurites [37]. The stimulation of rat pheochrocytoma PC12 cells with nerve growth factor (NGF) or serum starvation of mouse neuroblastoma N1E-115 cells reportedly caused neurite formation by upregulating Rac1 and CDC42 activities but was retarded by the dominant negative forms of Rac1 and CDC42 [38,39]. In another study, blocking Rac1 affected the axon growth of the Drosophila neuron [40]. Forced expression of the constitutively activated form of Rac1 facilitated the neurite outgrowth in rat hippocampal neurons [41]. By contrast, inhibition of RhoA by dominant negative RhoA or by RhoA inhibitor resulted in neurite outgrowth in mouse neural stem cells [42], whereas constitutively active RhoA attenuated the neurite outgrowth induced by NGF, BDNF, and neurotrophin 3 [43]. In line with these observations, our findings demonstrate that the wild-type, but not truncated forms, of *diras1* elevated the activities and protein level of Rac1, decreased the RhoA protein level, and subsequently triggered neuronal differentiation in Neuro-2a cells. Either the dominant negative Rac1 or the constitutively active RhoA blocked the *diras1*-induced neuronal polarization. Taken as a whole, our results suggest that *diras1* genes promote neuronal differentiation by modulating Rac1 and RhoA.

However, the molecular mechanisms underlying the *diras1*-dependent reduction of RhoA remain under investigation.

Evidence indicates that Pak1 regulates neuronal dynamics [30]. GTP-bound active Rac1 interacts with the N-terminal region of Pak1, which stimulates Pak1 activity. This condition triggers cytoskeleton reorganization, which results in neurite outgrowth in neuronal cells [30]. The constitutively active Pak1 enhances neurite number, whereas the dominant negative Pak1 attenuates neurite number in cortical neuron cells [44]. *Hayashi et al*. demonstrated that dominant negative Pak1 significantly decreased constitutively active Rac1-induced neurites in cultured pyramidal neurons [44]. In another study, *Tahirovic et al*. demonstrated that Pak1 activities were abolished in cerebella isolated from Rac1 knockout [33]. In line with these observations, we showed that dominant negative Pak1 reduced neuronal differentiation in *diras1a*- or *diras1b*-overexpressing Neuro-2a cells. Interestingly, no significant alternation of the phosphorylation of cofilin, a substrate of Pak1, was found in cells with and without *diras1* overexpression (data not shown). A previous report has shown that Rac2, but not Rac1, is involved in the dephosphorylation of cofilin in response to formyl-methionyl-leucyl-phenylalanine receptor activation [45]. Altogether, our data suggest that Pak1, but not cofilin activity, serves a crucial function in *diras1*-mediated actin cytoskeleton rearrangement.

CDK5 and its associated protein, p35, were shown to serve critical functions in the formation of neurite outgrowth during neuron differentiation [28]. CDK5/p35 also develops complex and active forms of Rac1 and can regulate actin cytoskeleton rearrangement [29]. Moreover, p35/CDK5/Rac1 complex was found to trigger actin cytoskeleton reorganization through hyperphosphorylation and Pak1 inhibition, eventually causing neurite outgrowth in cultured neuronal cells [29,46]. In this study, dominant negative CDK5 also blocked *diras1*-induced polarization in Neuro-2a cells. Our collective findings reveal that CDK5 is involved in the *diras1*-mediated neuronal differentiation as a downstream target of Rac1.

Reports also show that the WAVE/Arp2/3 pathways are involved in the Rac1-mediated actin cytoskeleton reorganization [47]. The WAVE regulatory complex binds to the active Rac1 and activates Arp2/3, thus causing actin polymerization [47]. *Miki et al*. have shown that WAVE interactes with Rac1 in Cos7 cells for the co-expression of WAVE and Rac1 [48]. The dominant negative WAVE inhibits the Rac1-induced membrane ruffling but does not affect the CDC42-induced spike-like formation [33]. Mislocalization of the WAVE in the cytosolic region was observed in the cerebellar granule neurons of Rac1 knockout mice [33]. The forced expression of WAVE overcame the defects in neuron polarization caused by the Rac1 knockout [33]. In this study, the forced expression of *diras1a* or *diras1b* stimulated the WAVE level, but not the alternation of Arp2/3 expression. However, CK-458 blocked Arp2/3 activities and diminished *diras1a* and *diras1b*-induced neuronal polarization. Our collective results indicate that the WAVE/Arp2/3 pathways may also be involved in the *diras1*-induced actin reorganization in neuronal cells.

In this study, the knockdown of *diras1a* and/or *diras1b* decreased the number of the trigeminal ganglion in zebrafish. More interestingly, *Kanungo et al*. demonstrated that the depletion of CDK5 expression by si-RNA reduced the primary sensory neurons of the trigeminal ganglion in zebrafish [49]. Our results suggest that CDK5 may function as a downstream effector of *diras1* genes. Thus, the knockdown of *diras1a* and/or *diras1b* may prevent CDK5 activity and subsequently decrease the trigeminal ganglion neurons. However, the overt alternation of the trigeminal ganglion precursor markers, such as *ngn1* and *neuroD,* was absent among the morphants and the control group at 11 hpf and 14 hpf, respectively. The lack of influence of *ngn1* and *neuroD* expressions in the early trigeminal ganglion of *diras1* morphants may be explained by the temporal expression patterns of *diras1a* and *diras1b*. The trigeminal ganglion precursor first appeared at 11 hpf as a small cluster of approximately 14 neurons, which reached 30 neurons at 24 hpf and consisted of approximately 55 neurons at 72 hpf [50]. *Caron et al*. showed that early-born and late-born trigeminal ganglions display distinct genes and functions [50]. However, *diras1a* and *diras1b* were rarely detectable before 12 hpf

when using RT-PCR and whole mount *in situ* hybridization. This finding suggests that both *diras1a* and *diras1b* are not essential for early trigeminal ganglion migration but may serve a critical function in neuron population.

This study is the first to demonstrate that zebrafish *diras1a* and *diras1b* promote neurite outgrowth in Neuro-2a cells and maintain trigeminal ganglion neurons in zebrafish. Both *diras1a* and *diras1b* enhance Rac1 levels and downregulate the RhoA level. Blocking Rac1 downstream targets significantly prevents the effects of *diras1a*- and *diras1b*-induced polarization in Neuro-2a cells. The depletion of *diras1a* and *diras1b* results in decreased trigeminal ganglion neurons. Such decrease can be restored by co-injection of mouse *Diras1* or constitutively active *Rac1* mRNA. In conclusion, our findings indicate that *diras1a* and *diras1b* are key factors in neurogenesis because of their cross-talks with other small GTPases, such as Rac1 and RhoA.

References

1. Colicelli J (2004) Human RAS superfamily proteins and related GTPases. Sci STKE 2004: RE13.
2. Mitin N, Rossman KL, Der CJ (2005) Signaling interplay in Ras superfamily function. Curr Biol 15: R563-574.
3. Wennerberg K, Rossman KL, Der CJ (2005) The Ras superfamily at a glance. J Cell Sci 118: 843-846.
4. Bourne HR, Sanders DA, McCormick F (1991) The GTPase superfamily: conserved structure and molecular mechanism. Nature 349: 117-127.
5. Ellis CA, Vos MD, Howell H, Vallecorsa T, Fults DW, et al. (2002) Rig is a novel Ras-related protein and potential neural tumor suppressor. Proc Natl Acad Sci U S A 99: 9876-9881.
6. Fukata M, Kaibuchi K (2001) Rho-family GTPases in cadherin-mediated cell-cell adhesion. Nat Rev Mol Cell Biol 2: 887-897.
7. Hall A (1998) Rho GTPases and the actin cytoskeleton. Science 279: 509-514.
8. Luo L (2000) Rho GTPases in neuronal morphogenesis. Nat Rev Neurosci 1: 173-180.
9. Ridley AJ, Paterson HF, Johnston CL, Diekmann D, Hall A (1992) The small GTP-binding protein rac regulates growth factor-induced membrane ruffling. Cell 70: 401-410.
10. Nobes CD, Hall A (1995) Rho, rac, and cdc42 GTPases regulate the assembly of multimolecular focal complexes associated with actin stress fibers, lamellipodia, and filopodia. Cell 81: 53-62.
11. Ridley AJ, Hall A (1992) The small GTP-binding protein rho regulates the assembly of focal adhesions and actin stress fibers in response to growth factors. Cell 70: 389-399.
12. Olenik C, Barth H, Just I, Aktories K, Meyer DK (1997) Gene expression of the small GTP-binding proteins RhoA, RhoB, Rac1, and Cdc42 in adult rat brain. Brain Res Mol Brain Res 52: 263-269.
13. Albertinazzi C, Gilardelli D, Paris S, Longhi R, de Curtis I (1998) Overexpression of a neural-specific rho family GTPase, cRac1B, selectively induces enhanced neuritogenesis and neurite branching in primary neurons. J Cell Biol 142: 815-825.
14. Brown MD, Cornejo BJ, Kuhn TB, Bamburg JR (2000) Cdc42 stimulates neurite outgrowth and formation of growth cone filopodia and lamellipodia. J Neurobiol 43: 352-364.
15. Yamashita T, Tucker KL, Barde YA (1999) Neurotrophin binding to the p75 receptor modulates Rho activity and axonal outgrowth. Neuron 24: 585-593.
16. Kontani K, Tada M, Ogawa T, Okai T, Saito K, et al. (2002) Di-Ras, a distinct subgroup of ras family GTPases with unique biochemical properties. J Biol Chem 277: 41070-41078.
17. Tada M, Gengyo-Ando K, Kobayashi T, Fukuyama M, Mitani S, et al. (2012) Neuronally expressed

Ras-family GTPase Di-Ras modulates synaptic activity in Caenorhabditis elegans. Genes Cells 17: 778-789.

18. Westerfield M, Doerry E, Kirkpatrick AE, Douglas SA (1999) Zebrafish informatics and the ZFIN database. Methods Cell Biol 60: 339-355.
19. Westerfield M, Doerry E, Kirkpatrick AE, Driever W, Douglas SA (1997) An on-line database for zebrafish development and genetics research. Semin Cell Dev Biol 8: 477-488.
20. Kimmel CB, Ballard WW, Kimmel SR, Ullmann B, Schilling TF (1995) Stages of embryonic development of the zebrafish. Dev Dyn 203: 253-310.
21. Thisse C, Thisse B (2008) High-resolution in situ hybridization to whole-mount zebrafish embryos. Nat Protoc 3: 59-69.
22. Hsu LS, Tseng CY (2010) Zebrafish calcium/calmodulin-dependent protein kinase II (cam-kii) inhibitors: expression patterns and their roles in zebrafish brain development. Dev Dyn 239: 3098-3105.
23. Hsu LS, Liang CJ, Tseng CY, Yeh CW, Tsai JN (2011) Zebrafish Cyclin-Dependent Protein Kinase–Like 1 (zcdkl1): Identification and Functional Characterization. Int J Mol Sci 12: 3606-3617.
24. Schmidt A, Hall A (2002) Guanine nucleotide exchange factors for Rho GTPases: turning on the switch. Genes Dev 16: 1587-1609.
25. Auer M, Hausott B, Klimaschewski L (2011) Rho GTPases as regulators of morphological neuroplasticity. Ann Anat 193: 259-266.
26. Manser E, Chong C, Zhao ZS, Leung T, Michael G, et al. (1995) Molecular cloning of a new member of the p21-Cdc42/Rac-activated kinase (PAK) family. J Biol Chem 270: 25070-25078.
27. Bokoch GM (2003) Biology of the p21-activated kinases. Annu Rev Biochem 72: 743-781.
28. Kesavapany S, Li BS, Pant HC (2003) Cyclin-dependent kinase 5 in neurofilament function and regulation. Neurosignals 12: 252-264.
29. Nikolic M, Chou MM, Lu W, Mayer BJ, Tsai LH (1998) The p35/Cdk5 kinase is a neuron-specific Rac effector that inhibits Pak1 activity. Nature 395: 194-198.
30. Kreis P, Barnier JV (2009) PAK signalling in neuronal physiology. Cell Signal 21: 384-393.
31. Pollard TD, Borisy GG (2003) Cellular motility driven by assembly and disassembly of actin filaments. Cell 112: 453-465.
32. Stradal TE, Scita G (2006) Protein complexes regulating Arp2/3-mediated actin assembly. Curr Opin Cell Biol 18: 4-10.
33. Tahirovic S, Hellal F, Neukirchen D, Hindges R, Garvalov BK, et al. (2010) Rac1 regulates neuronal polarization through the WAVE complex. J Neurosci 30: 6930-6943.
34. Knaut H, Blader P, Strahle U, Schier AF (2005) Assembly of trigeminal sensory ganglia by chemokine signaling. Neuron 47: 653-666.
35. Oxford G, Theodorescu D (2003) Ras superfamily monomeric G proteins in carcinoma cell motility. Cancer Lett 189: 117-128.
36. Cheever TR, Ervasti JM (2013) Actin isoforms in neuronal development and function. Int Rev Cell Mol Biol 301: 157-213.
37. Govek EE, Newey SE, Van Aelst L (2005) The role of the Rho GTPases in neuronal development. Genes Dev 19: 1-49.
38. Aoki K, Nakamura T, Matsuda M (2004) Spatio-temporal regulation of Rac1 and Cdc42 activity during

nerve growth factor-induced neurite outgrowth in PC12 cells. J Biol Chem 279: 713-719.
39. Sarner S, Kozma R, Ahmed S, Lim L (2000) Phosphatidylinositol 3-kinase, Cdc42, and Rac1 act downstream of Ras in integrin-dependent neurite outgrowth in N1E-115 neuroblastoma cells. Mol Cell Biol 20: 158-172.
40. Luo L, Liao YJ, Jan LY, Jan YN (1994) Distinct morphogenetic functions of similar small GTPases: Drosophila Drac1 is involved in axonal outgrowth and myoblast fusion. Genes Dev 8: 1787-1802.
41. Schwamborn JC, Puschel AW (2004) The sequential activity of the GTPases Rap1B and Cdc42 determines neuronal polarity. Nat Neurosci 7: 923-929.
42. Gu H, Yu SP, Gutekunst CA, Gross RE, Wei L (2013) Inhibition of the Rho signaling pathway improves neurite outgrowth and neuronal differentiation of mouse neural stem cells. Int J Physiol Pathophysiol Pharmacol 5: 11-20.
43. Da Silva JS, Medina M, Zuliani C, Di Nardo A, Witke W, et al. (2003) RhoA/ROCK regulation of neuritogenesis via profilin IIa-mediated control of actin stability. J Cell Biol 162: 1267-1279.
44. Hayashi K, Ohshima T, Hashimoto M, Mikoshiba K (2007) Pak1 regulates dendritic branching and spine formation. Dev Neurobiol 67: 655-669.
45. Sun CX, Magalhaes MA, Glogauer M (2007) Rac1 and Rac2 differentially regulate actin free barbed end formation downstream of the fMLP receptor. J Cell Biol 179: 239-245.
46. Rashid T, Banerjee M, Nikolic M (2001) Phosphorylation of Pak1 by the p35/Cdk5 kinase affects neuronal morphology. J Biol Chem 276: 49043-49052.
47. Takenawa T, Miki H (2001) WASP and WAVE family proteins: key molecules for rapid rearrangement of cortical actin filaments and cell movement. J Cell Sci 114: 1801-1809.
48. Miki H, Suetsugu S, Takenawa T (1998) WAVE, a novel WASP-family protein involved in actin reorganization induced by Rac. EMBO J 17: 6932-6941.
49. Kanungo J, Li BS, Goswami M, Zheng YL, Ramchandran R, et al. (2007) Cloning and characterization of zebrafish (Danio rerio) cyclin-dependent kinase 5. Neurosci Lett 412: 233-238.
50. Caron SJ, Prober D, Choy M, Schier AF (2008) In vivo birthdating by BAPTISM reveals that trigeminal sensory neuron diversity depends on early neurogenesis. Development 135: 3259-3269.

Acknowledgements

These authors thank Dr. Yi-Shuian Huang (Institute of Biomedical Sciences, Academia Sinica, Taipei, Taiwan) for provided pCMV-mCherry plasmid and Addgene for provided plasmids as mentioned in “Material and methods” section. This study was supported by grants obtained from the Ministry of Science and Technology of Taiwan (MOST-103-2311-B-040-001). The authors thank the Zebrafish Core in Academia Sinica (ZCAS), Institute of Cellular and Organismic Biology (ICOB), which is supported by grant NSC-103-2321-B-001-050 from the National Science Council (NSC), the Taiwan Zebrafish Core Facility (TZCF) for providing the zebrafish AB strain and *Tg*(*huc:gfp*), and the National Health Research Institute (NHRI), which is supported by grant 100-2321-B-400-003 from National Science Council (NSC). Upright fluorescent microscopy was performed in the Instrument Center of Chung Shan Medical University, which is supported by the National Science Council, Ministry of Education and Chung Shan Medical University.

Conflicts of Interest These authors declare that there are no conflicts of interest.

FIGURE LEGENDS

Fig. 1. Protein sequence alignments, phylogenetic tree and expression patterns of zebrafish *diras1a* and *diras1b*. (a) Multiple alignments of *diras1a* and *diras1b* amino acid sequences were compared with those of human (*H-DI-Ras1*), mouse (*M-DI-Ras1*), rat (*R-DI-Ras1*), and *Xenopus* (*X-DI-Ras1*). The *DIRAS1* sequences from the five species were aligned using ClustalW. Identical sequences are shaded in yellow, whereas residue similarities of the four *DIRAS1* proteins are presented in cyan. (b) A phylogenetic tree was constructed based on the multiple alignments of the DIRAS1 proteins using MegAlign in DNASTAR through the neighbor joining method. Scale bars indicate nucleotide substitutions (100×). (c) A graphical representation of the conserved synteny of the *DIRAS1* gene clusters in human chromosome 19, rat chromosome 7, mouse chromosome 10, and zebrafish linking groups (LG) 2. The *diras1a* gene is localized in LG 11. Ch denotes the chromosome. Whole mount *in situ* hybridization was performed using antisense riboprobes against *diras1a* (d) and *diras1b* (e) at the indicated developmental stages. The stages of embryonic development are indicated in the right (d,e). di: diencephalon, GCL: ganglion cell layer, H.B.: hindbrain, and tel: telencephalon. Stages are indicated in the upper right.

Fig. 2. Zebrafish *diras1* enhanced neurite outgrowth in Neuro-2a cells. (a,b) Neuro-2a cells were transiently transfected with pEGFP vectors, namely, pEGFP-*diras1a*, pEGFP-*diras1b*, pEGFP-*diras1a*-ct, or pEGFP-*diras1b*-ct. The cells were fixed at 24 h post-transfection, and the actin cytoskeleton was stained with rhodamine/phalloidin (in red) (a) to determine the percentage of cells with neurite outgrowth. The *arrowhead* indicates lamellipodia-like structure. The *arrow* indicates protrusion formation. (b). *Scale bars* (a): 50 μm. The nucleus was stained with DAPI (in blue). Data are presented as the mean ± S.D. of three independent experiments. ***$p < 0.001$ (Student's *t* test).

Fig. 3. Functional characterization of zabrafish *diras1a* and *diras1b*. (a) Neuro-2a cells were transfected with pEGFP vectors, namely, pEGFP-*diras1a*, pEGFP-*diras1b*, pEGFP-*diras1a*-ct, or pEGFP-*diras1b*-ct. The protein levels of Rac1, Cdc42, and RhoA were detected using Western blot analysis. β-Actin was used for normalization. (b) Data are presented as the mean ± S.D. of three independent experiments. *$p < 0.05$; **$p < 0.01$. (c) Rac1 activity was assessed by extracting GTP-bound Rac1 proteins from cell lysates using the GST-Pak1-PBD fusion protein. About 500 μg of lysates derived from cells transfected with the indicated plasmids were incubated with GST-Pak1-PBD or GST alone. After the pull-down assay, Rac1 was detected with immunoblotting. Whole input lysate was detected with an anti-GFP antibody. Coomassie blue-stained SDS-PAGE gels show the molecular weight of the GST and the GST-Pak1-PBD fusion protein.

Fig. 4. Rac1 inactivation, RhoA activation, Pak1 inhibition, or CDK5 inhibition blocked *diras1*-induced neurite outgrowth. (a,b) Neuro-2a cells were co-transfected with pEGFP-*diras1a* or pEGFP-*diras1b* combined with pYFP vector or pYFP-dominant negative Rac1 (T17N). The cells were fixed and stained with rhodamine/phalloidin (in red) at 24 h post-transfection to examine the percentage of neuronal cell differentiation (b). Neuro-2a cells were co-transfected with pEGFP-*diras1a* or pEGFP-*diras1b* combined with pCMV-mCherry vector or pCMV-mCherry-constitutive activated RhoA (Q63L), pCMV-mCherry-catalytically inactivated Pak1 (K299R) or pCMV-mCherry-dominant negative CDK5 (D145N) for 24 h. The cells were fixed, and the neurite outgrowth rate was examined. Images show the morphology of the cells (c). The panel shows the percentages of cell differentiation (d). *Scale bars* (a,c): 50 μm. The nucleus was stained with DAPI (in blue). Data are presented as the mean ± S.D. of three independent experiments. ***$p < 0.001$ (Student's *t* test).

Fig. 5. WAVE and Arp2/3 were involved in *diras1*-mediated neurite outgrowth. (a) Neuro-2a cells were transfected with pEGFP vectors, namely, pEGFP-*diras1a*, pEGFP-*diras1b*, pEGFP-*diras1a*-ct, or pEGFP-*diras1b*-ct. The protein levels of WAVE and Arp2/3 were detected using Western blot analysis. β-Actin was used for normalization. (b) Data

are presented as the mean ± S.D. of three independent experiments. (c,d) Neuro-2a cells with or without pre-treatment with Arp2/3 inhibitor (CK-548) were transfected with pEGFP vectors, namely, pEGFP-*diras1a* or pEGFP-*diras1b*. The cells were fixed and stained with rhodamine/phalloidin (in red) at 24 h post-transfection to investigate morphological changes. The nucleus was stained with DAPI (in blue). *Scale bars* (c): 50 μm. Data are presented as the mean ± S.D. of three independent experiments. ***$p < 0.001$ (Student's *t* test).

Fig. 6. Effects of *diras1* gene depletion on neurogenesis using the *Tg*(*huC*:*gfp*) model. The embryos that received the indicated MOs were collected at 48 hpf. The expression of *huC* was abrogated in *diras1* morphants. Reduced trigeminal sensory ganglion territories were also observed in *diras1* morphants. The deficiency in *huC* expression was restored via co-injection with the wild-type but not with the C-terminus truncated form of mouse *Diras1 m*RNA. All images are shown in lateral view. *Scale bars*: 100 μm. Tc: telencephalic cluster, Tg: trigeminal ganglion, Tec: tectum, and Hb: hindbrain.

Fig. 7. Effects of *diras1* depletion on neurogenesis as visualized using acetylated tubulin (AcTub) and islet1/2 staining. (a) AcTub expression (an axonal marker) was examined using confocal microscopy at 24 hpf. The axonal scaffolds of the trigeminal sensory ganglion in *diras1* morphants were visibly curtailed. Co-injection with the wild-type but not with the C-terminus truncated form of mouse *Diras1* mRNA restored the neurons of the trigeminal ganglion. The *arrowhead* indicates the trigeminal sensory ganglion. (b) Embryos that received the indicated MO were collected at 24 hpf. The trigeminal sensory ganglion was marked using an islet1/2 antibody via immunostaining. Trigeminal sensory ganglia decreased in *diras1a* and *diras1b* morphants. These defects can be restored by mouse *Diras1* mRNA. All images are shown in lateral view. *Scale bars*: 100 μm. (c) Data are presented as the mean ± S.D. of three independent experiments. *$p < 0.05$, the morphant group compared with the control MO; #$p < 0.05$, co-injection with the wild-type mRNA group compared with the morphant group (Student's *t* test). *Scale bars* (a,b): 100 μm.

Fig. 8. Knockdown of *diras1* did not impair the positioning of the trigeminal sensory ganglion. (a,b) The embryos that received the indicated MO with or without the corresponding RNA were collected. Whole mount *in situ* hybridization for *ngn1* expression at 11 hpf (a) and *neuroD* expression at 14 hpf (b) was performed. Trigeminal sensory ganglia were settled in small clusters at 11 hpf and formed compact clusters at 14 hpf. This arrangement is indistinguishable between the control and morphants. Precursors of the trigeminal sensory ganglion (tg) are indicated. All images are in dorsal view with the anterior at the top. *Scale bars* (a,b): 100 μm.

Fig. 9. Zebrafish *diras1* was required for trigeminal sensory gangliongenesis through the Rac1-dependent pathway. (a) The morphants that received the indicated MOs were collected at 24 hpf. An islet1/2 antibody was used as a marker of the trigeminal sensory ganglion. Trigeminal sensory ganglia decreased in *diras1a* or/and *diras1b* morphants. These defects can be restored by injecting the constitutive activation of *Rac1* mRNA. All images are shown in lateral view. *Scale bars* (a): 100 μm. (b) Quantitative analyses of islet1/2-positive neurons are presented as the mean ± S.D. of three independent experiments. *$p < 0.05$, the morphant group compared with the control MO; #$p < 0.05$, co-injection with the wild-type mRNA group compared with the morphant group (Student's *t* test).

Fig. S1. Neuro-2a cells were transfected with inhibitory constructs alone and did not cause morphological change. Neuro-2a cells were transiently transfected with various inhibitory constructs. Data are presented as the mean ± S.D. of three independent experiments.

Fig. S2. Specificity of *diras1a* and *diras1b* morpholinos. Two GFP reporter plasmids (*diras1a:gfp* and *diras1b:gfp*) that encompass the MO target sequences were constructed. Embryos that received 100 pg of *diras1a:gfp* or *diras1b:gfp* showed a mosaic GFP expression at 24 hpf. Co-injection of *diras1a:gfp* or *diras1b:gfp* with the corresponding MO but not the five-mismatched MOs significantly diminished GFP expression. *Scale bars*: 1 mm.

Fig. S3. Zebrafish *diras1a* and *diras1b* splice morpholino (Sp-MO) effectively blocked the correct splicing of pre-mRNA without compensation effects. (a) Schematic indicates the intron and exon structures and position of Sp-MO (red) and RT-PCR primers (arrows). (b) Embryos were injected at the single-cell stage with *diras1a* and/or *diras1b* Sp-MO. RNAs were extracted and analyzed using RT-PCR. Corrected splicing fragments were found in the control MO groups but not in the *diras1a* and/or *diras1b* Sp-MO groups. Lane 1: marker, lane 2: control MO, lane 3: control MO, lane 4: *diras1a*-Sp-MO, lane 5: *diras1b*-Sp-MO, lane 6: *diras1a*- and *diras1b*-Sp-MO. (c) RT-PCR analyses of the *diras1a* and *diras1b* gene in *diras1* morphants suggested that the knockdown of *diras1a* or *diras1b* did not induce the complementary effect. Lane 1: marker, lane 2: control MO, lane 3: *diras1a*-Sp-MO, lane 4: control MO, lane 5: *diras1b*-Sp-MO. Elongation factor 1α was used as the internal control.

Fig. S4. Loss of the **trigeminal ganglion** in *diras1a* and/or *diras1b* **Sp-MO morphants.** (a) The embryos that received the indicated Sp-MO were collected at 24 hpf. The trigeminal sensory ganglion was marked using an islet1/2 antibody via immunostaining. All images are shown in lateral view. *Scale bars*: 100 μm. (b) Quantitative analyses of islet1/2-positive neurons are presented as the mean ± S.D. of three independent experiments. $*p < 0.05$, the morphant group compared with the control MO (Student's *t* test).

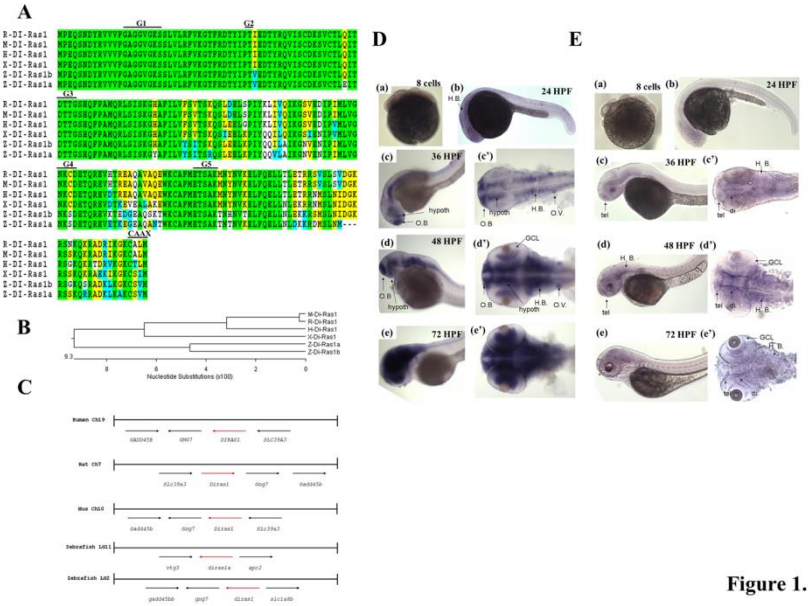

Figure 1.

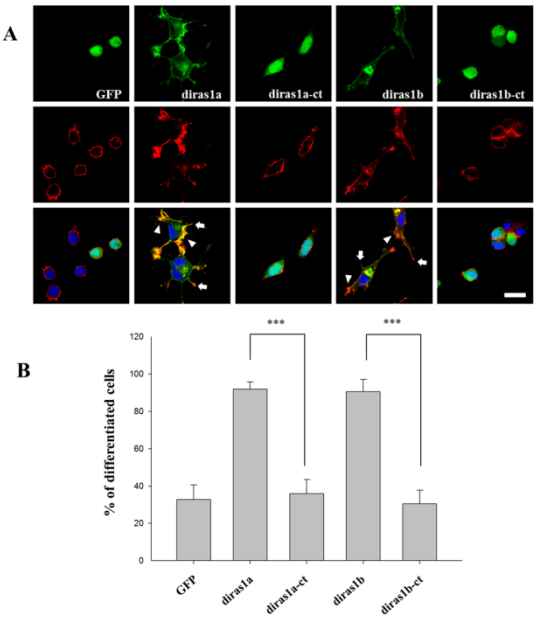

Figure 2.

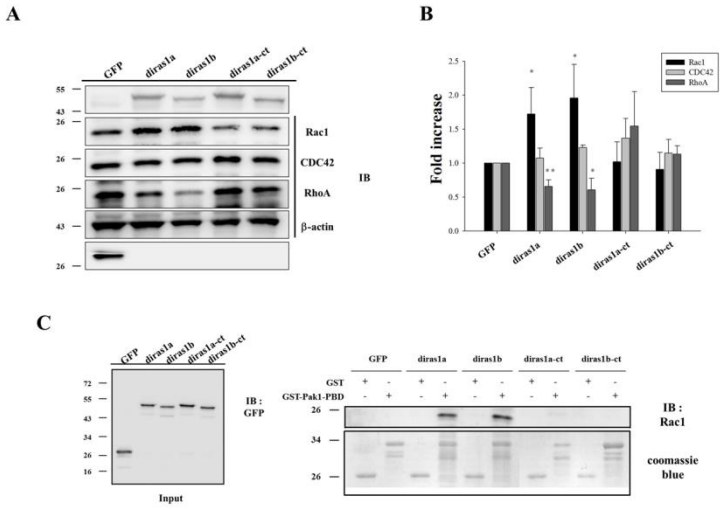

Figure 3.

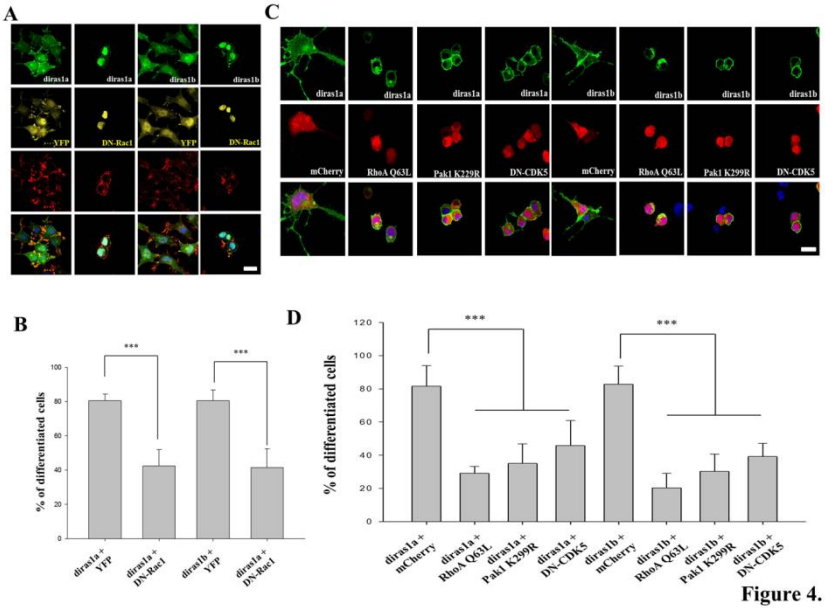

Figure 4.

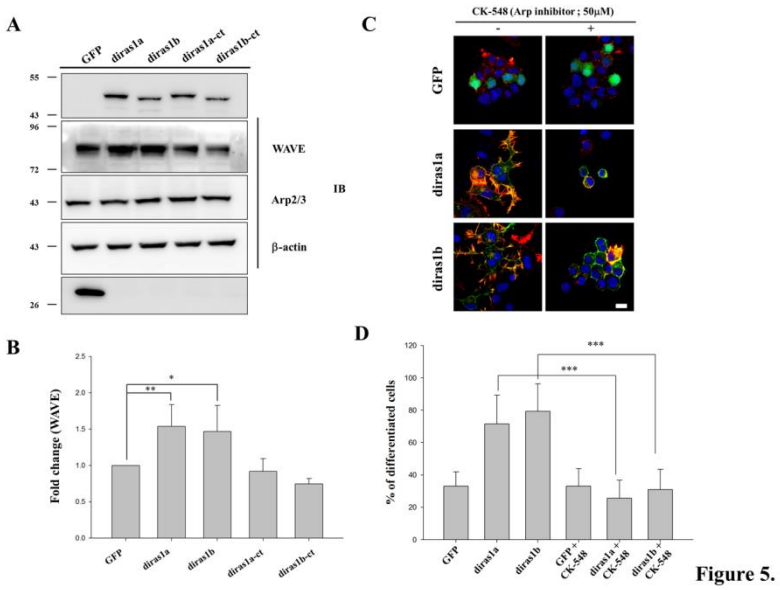

Figure 5.

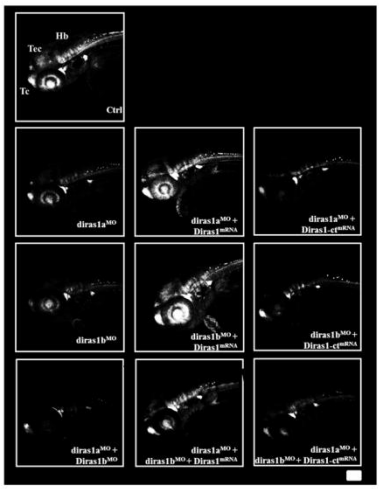

Figure 6.

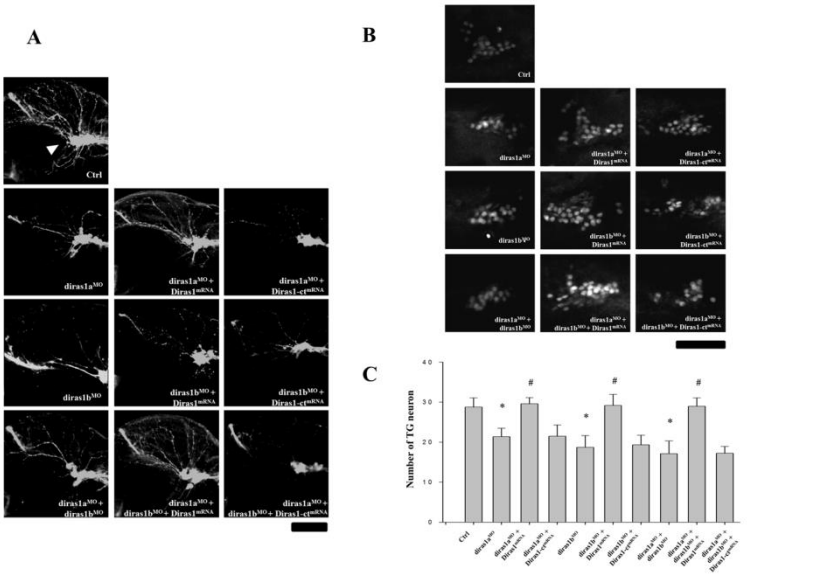

Figure 7.

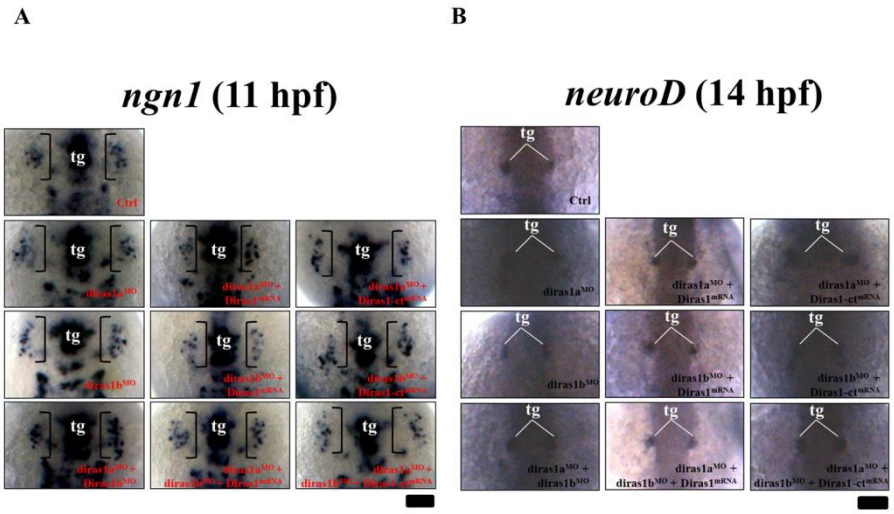

Figure 8.

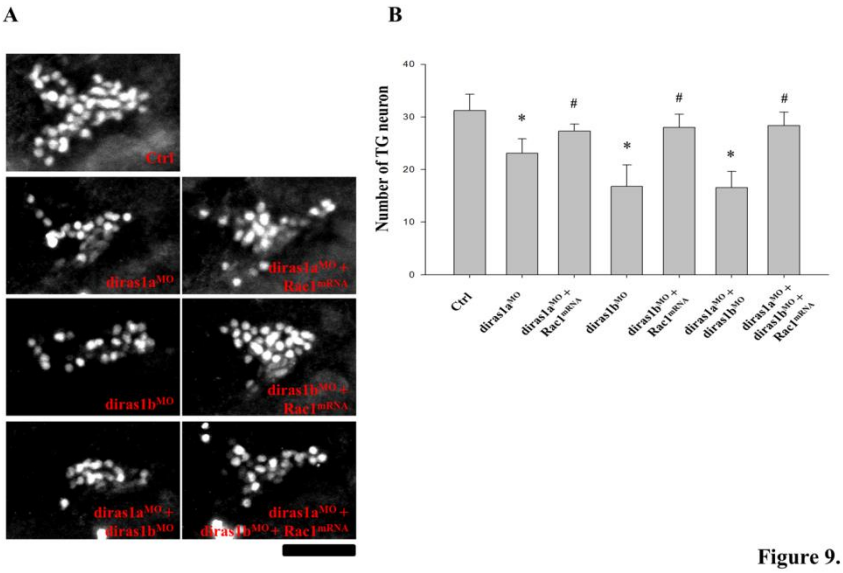

Figure 9.

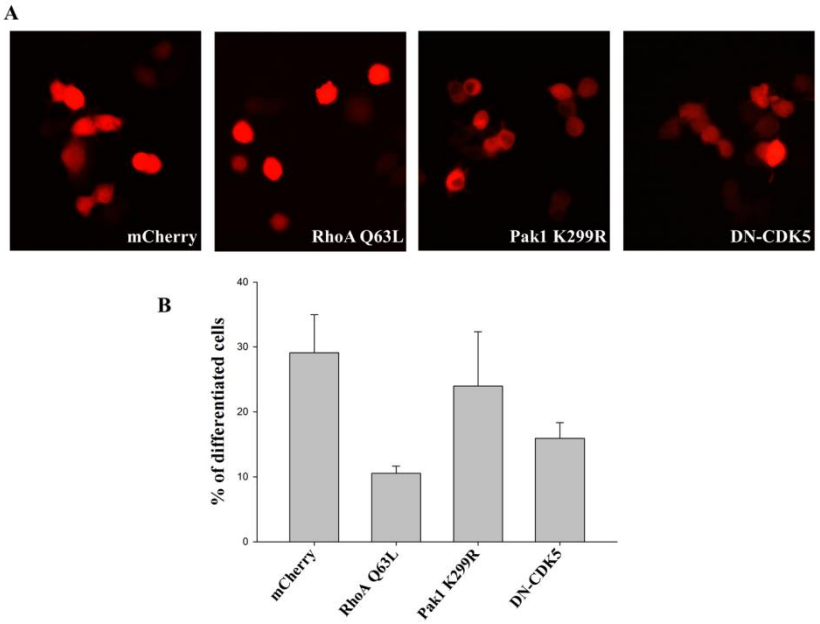

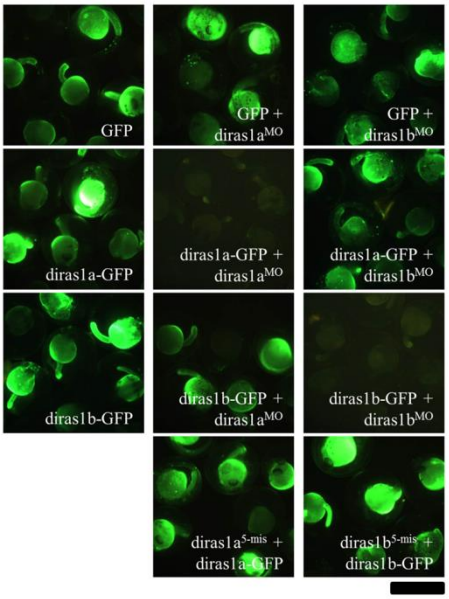
GFP
GFP + diras1a^MO
GFP + diras1b^MO
diras1a-GFP
diras1a-GFP + diras1a^MO
diras1a-GFP + diras1b^MO
diras1b-GFP
diras1b-GFP + diras1a^MO
diras1b-GFP + diras1b^MO
diras1a^5-mis + diras1a-GFP
diras1b^5-mis + diras1b-GFP

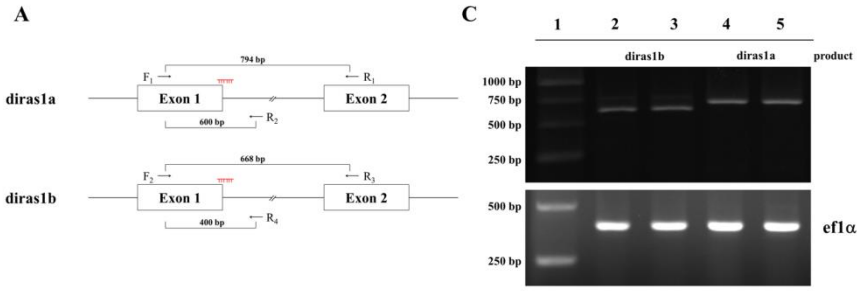
A
diras1a
794 bp
F1
R1
Exon 1
Exon 2
600 bp
R2
diras1b
668 bp
F2
R3
Exon 1
Exon 2
400 bp
R4
C
1 2 3 4 5
diras1b
diras1a
product
1000 bp
750 bp
500 bp
250 bp
500 bp
250 bp
ef1α

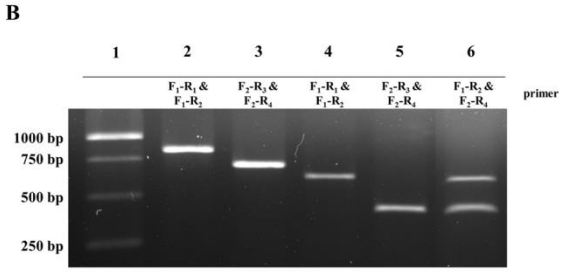
B
1 2 3 4 5 6
F1-R1 & F1-R2
F2-R3 & F2-R4
F1-R1 & F1-R2
F2-R3 & F2-R4
F1-R2 & F2-R4
primer
1000 bp
750 bp
500 bp
250 bp

四、建議

國內應多加舉辦如此大型會議、增加補助出國額度、或盡量補助博士班學生出國開會或短期研究之經費，讓年輕研究學者有機會與大師級學者學習。

五、攜回資料名稱及內容

會議議程手冊

展示廠商資料

會議摘要手冊

六、其他

感謝科技部贊助與支持學專家出國開會,更能拓展其在研究領域上有不同的視野及想法。

科技部補助計畫衍生研發成果推廣資料表

日期:2015/10/11

科技部補助計畫	計畫名稱: 探討斑馬魚di-ras基因及其相關基因在神經發育所扮演的角色
	計畫主持人: 許立松
	計畫編號: 103-2311-B-040-001- 學門領域: 生物學之生化及分子生物

無研發成果推廣資料

103年度專題研究計畫研究成果彙整表

計畫主持人：許立松	**計畫編號：**103-2311-B-040-001-
計畫名稱：探討斑馬魚di-ras基因及其相關基因在神經發育所扮演的角色	

成果項目			量化			單位	備註（質化說明：如數個計畫共同成果、成果列為該期刊之封面故事...等）
			實際已達成數（被接受或已發表）	預期總達成數（含實際已達成數）	本計畫實際貢獻百分比		
國內	論文著作	期刊論文	0	0	100%	篇	
		研究報告/技術報告	0	0	100%		
		研討會論文	0	0	100%		
		專書	0	0	100%	章/本	
	專利	申請中件數	0	0	100%	件	
		已獲得件數	0	0	100%		
	技術移轉	件數	0	0	100%	件	
		權利金	0	0	100%	千元	
	參與計畫人力（本國籍）	碩士生	0	0	100%	人次	
		博士生	0	0	100%		
		博士後研究員	0	0	100%		
		專任助理	1	1	100%		
國外	論文著作	期刊論文	0	0	100%	篇	此論文正在審稿中
		研究報告/技術報告	0	0	100%		
		研討會論文	1	1	100%		
		專書	0	0	100%	章/本	
	專利	申請中件數	0	0	100%	件	
		已獲得件數	0	0	100%		
	技術移轉	件數	0	0	100%	件	
		權利金	0	0	100%	千元	
	參與計畫人力（外國籍）	碩士生	0	0	100%	人次	
		博士生	0	0	100%		
		博士後研究員	0	0	100%		
		專任助理	1	1	100%		
其他成果（無法以量化表達之成果如辦理學術活動、獲得獎項、重要國際合作、研究成果國際影響力及其他協助產業技術發展之具體效益事項等，請以文		無					

字敘述填列。）	

	成果項目	量化	名稱或內容性質簡述
科教處計畫加填項目	測驗工具(含質性與量性)	0	
	課程/模組	0	
	電腦及網路系統或工具	0	
	教材	0	
	舉辦之活動/競賽	0	
	研討會/工作坊	0	
	電子報、網站	0	
	計畫成果推廣之參與（閱聽）人數	0	

科技部補助專題研究計畫成果報告自評表

請就研究內容與原計畫相符程度、達成預期目標情況、研究成果之學術或應用價值（簡要敘述成果所代表之意義、價值、影響或進一步發展之可能性）、是否適合在學術期刊發表或申請專利、主要發現或其他有關價值等，作一綜合評估。

1. 請就研究內容與原計畫相符程度、達成預期目標情況作一綜合評估
   ■達成目標
   □未達成目標（請說明，以100字為限）
   　□實驗失敗
   　□因故實驗中斷
   　□其他原因
   說明：

2. 研究成果在學術期刊發表或申請專利等情形：
   論文：□已發表 ■未發表之文稿 □撰寫中 □無
   專利：□已獲得 □申請中 ■無
   技轉：□已技轉 □洽談中 ■無
   其他：（以100字為限）
   目前此研究成果正投稿漁Molecular Neurobiology且在revised中

3. 請依學術成就、技術創新、社會影響等方面，評估研究成果之學術或應用價值（簡要敘述成果所代表之意義、價值、影響或進一步發展之可能性）（以500字為限）
   此研究成果顯示在斑馬魚中剃除diraslа或是diraslb基因會造成斑馬魚中trigeminal ganlion 的數目減少並且此機轉是透過Racl的訊號傳遞,我們的結果可以提供日後研究trigeminal ganglion缺陷的疾病是否由diras1缺損所引起的.